

**A Comparison of Durability and Recruitment for  
Reef Mimics Constructed from Marine Concrete and  
CaCO<sub>3</sub>-Enriched Concrete**

by

Georgette L. Tso

B.S. Mechanical Engineering  
Massachusetts Institute of Technology, 2019

Submitted to the Department of Civil and Environmental Engineering in  
partial fulfillment of the requirements for the degree of

Master of Engineering in the Environmental Engineering Science

at the

MASSACHUSETTS INSTITUTE OF TECHNOLOGY

February 2021

© Massachusetts Institute of Technology 2021. All rights reserved.

Author

.....  
Department of Civil and Environmental Engineering  
January 15, 2021

Certified by

.....  
Heidi M. Nepf  
Donald and Martha Harleman Professor of Civil and Environmental  
Engineering  
Thesis Supervisor

Accepted by

.....  
Colette M. Heald  
Professor of Civil and Environmental Engineering  
Chair, Graduate Program Committee

# A Comparison of Durability and Recruitment for Reef Mimics Constructed from Marine Concrete and CaCO<sub>3</sub>-Enriched Concrete

by

Georgette L. Tso

Submitted to the Department of Civil and Environmental Engineering  
on January 15, 2020

in partial fulfillment of the requirements for the degree of  
Master of Engineering in the Environmental Engineering Science

## Abstract

Coastal landscapes continue to be altered on a global scale by man-made infrastructure. Coastal and marine infrastructure, such as seawalls, breakwaters, have replaced natural intertidal, subtidal, and benthic habitats along many coastlines. Coastal infrastructure has a multitude of impacts on biodiversity and ecosystem functioning. The habitat provided by man-made coastal infrastructure typically supports ecological communities that are characterized by greater abundances of invasive species and lower overall biodiversity. New design approaches have emerged with the aim of mitigating the impacts of man-made coastal infrastructure, but few studies have investigated the role of CaCO<sub>3</sub> as a concrete additive in increasing biodiversity, species recruitment, material strength and durability, and ion leaching. Textured reef mimics in both standard marine concrete and CaCO<sub>3</sub>-enriched concrete were studied constructed and deployed along the coast in Dorchester Bay, Massachusetts. Reef mimics were compared with regard to performance in recruitment and durability at 90, 180, 330, and 420 days to evaluate effect of CaCO<sub>3</sub> and correlations with seasonal influences over a 420-day period. CaCO<sub>3</sub> had limited effect on community structure as a whole, but increased mussel recruitment, mussel size, and increased barnacle and common slipper shell recruitment on the innermost disc surface. Community structure varied more with submersion time than material type. Community structure varied in time with boom-bust cycles, where the invasive ascidians *S. clava*, *A. aspersa*, *B. violaceus*, and *Didemnum* sp. competed for surface coverage. CaCO<sub>3</sub> did not decrease the compressive strength or durability of concrete reef mimics. Submersion caused a decrease in compressive strength of both standard and enriched concretes, but after the initial decrease, compressive strength increased with submersion time in the field, but never recovered to its original strength. Although CaCO<sub>3</sub>-enriched concrete leached higher concentrations of calcium and carbonate ions, reef mimics of both material types demonstrated the ability to provide continued leaching of ions.

Thesis Supervisor: Heidi M. Nepf

Title: Donald and Martha Harleman Professor of Civil and Environmental Engineering



# Acknowledgements

Thank you, Heidi, for taking me on advising my research first as an undergraduate researcher and then as a graduate student. Thank for the mentorship and guidance you have given me since we met in late 2018 and throughout my degree, including the difficult pandemic period.

Thank you, Dr. Carolina Bastidas, for your mentorship in marine biology concepts, tools, and laboratory techniques. Thank you also for your willingness to guide me in a field new to me and for your time and generosity.

Thank you, Francesco Peri, for your immense support in designing, engineering, and implementing our field experiments. I will cherish the memories I have working outdoors during both hot summers and rainy winters at Fallon Pier.

Thank you, Steve Rudolph, for your time and support in conducting material testing at your lab.

Thank you, Juliet Simpson and MIT SeaGrant, for your generosity in sharing laboratory space and tools.

Thank you, Mom and Dad, for everything!





# Contents

<b>1 Introduction</b>	<b>16</b>
1.1 Motivation.....	16
1.2 Project Overview.....	18
<b>2 Background</b>	<b>20</b>
2.1 Seawalls versus natural intertidal, subtidal, and benthic habitats.....	20
2.2 Mollusk species as ecosystem engineers and concrete fortifiers.....	21
2.3 Standard marine concrete: physical and chemical properties, material strength and durability, and calcium ion leaching potential.....	22
2.4 Intertidal, subtidal, and benthic marine habitats and species of Boston Harbor Islands National Park.....	24
2.5 The calcium carbonate dissolution-precipitation reaction.....	26
2.6 Impact of increasing atmospheric CO <sub>2</sub> on shelled organisms.....	27
2.7 Calcium carbonate precipitation in mollusk shells.....	28
2.8 Factors influencing biodiverse recruitment: chemical cues, biofilms, flow conditions, substrate surface topography.....	29
2.9 Calcium carbonate dissolution from a concrete plate.....	34
<b>3 Methods</b>	<b>38</b>
3.1 Experimental Methodology.....	38
3.1.1. Artificial habitat structures.....	38

3.1.2. Field site and permitting.....	41
3.1.3. Field treatment design.....	42
3.1.4. Disc material testing.....	45
3.1.5. Disc identification.....	48
3.1.6. Construction of hanging research structures.....	49
3.1.7. Deployment and retrieval of hanging research structures on John T. Fallon State Pier.....	52
3.1.8. Sampling.....	53
3.1.9. Flume experiments to measure CaCO <sub>3</sub> leaching from discs.....	54
3.2 Statistical Analysis.....	57
3.2.1. Bray-Curtis similarity matrix.....	57
3.2.2. Non-metric Multidimensional Scaling (nMDS).....	58
3.2.3. SIMPER analysis.....	58
3.2.4. Independent t-tests.....	58
<b>4 Results</b>	<b>60</b>
4.1 Observations from Field Deployment.....	61
4.2 Percent Cover.....	63
4.2.1. Top Surface Layer.....	63
4.2.2. Innermost Surface Layer.....	67
4.3 Multivariate Analysis.....	69
4.4 Flume Experimentation.....	71
4.5 Material Testing.....	76
<b>5 Discussion</b>	<b>81</b>
<b>6 Summary</b>	<b>91</b>
<b>7 Sources</b>	<b>93</b>



# List of Figures

- 2.1 Figure 2.1: Map of the Boston Harbor Islands national park area with the ten largest islands labelled by name, and with the field site marked in red. Boston Harbor Islands national park area is comprised of 34 total islands in Massachusetts Bay, the same bay in which our field site was located. 25
- 2.2 Concentrations of the three dissolved inorganic carbon species are dependent on pH. As ocean acidification progresses, oceanic pH decreases, and the concentration of carbonate ion decreases, putting shelled organisms who rely on calcium and carbonate ions at risk. 28
- 3.1 The artificial habitat structures are discs with a 2.5” height, a 4” diameter, and a 1.25” diameter center hole. The center hole facilitates deployment by allowing discs to be strung onto ropes, chains, or pipes. 39
- 3.2 The lateral surfaces of the discs are textured to facilitate recruitment of biodiverse growth. The lateral surface of the discs is textured with two rows of evenly spaced hemispherical cavities that are 0.8” in diameter, 0.25” in depth from the lateral surface, and 0.2” apart. The inner surfaces of each hemispherical cavity were further textured with a knife and re-packed with concrete clumps. Additionally, aggregates up to 0.1875” in diameter in the concrete mixture contributed to a randomly bumpy overall surface texture. 40
- 3.3 A diagram of the experimental setup at Fallon Pier. The vertical blue rectangles represent all eight research structures and their total lengths from the bottom of Fallon Pier to the bed. Research structures were hung with galvanized steel chain. The gray rectangles represent the discs. The light blue horizontal lines mark where mean high tide and mean low tide levels are relative to the pier and to the research structures. The discs were deployed such that they would always be submerged. A 6-foot human figure is included for comparison. 44
- 3.4 South-facing side of Fallon Pier with Research Structure #3 and #4 hung from wooden railing posts with 1 m distance in between. 45
- 3.5 The rebound hammer (blue) is applied four times at four equidistant points (red dots) on the top surface (not the lateral surface) of each disc. Gentle manual force on the end of the rebound 46

hammer activates the internal spring, which impacts the concrete and displays a rebound number.	
3.6 Correlation curve for the Humboldt Manufacturing H-2975L Schmidt Hammer, Type L on GROW and control material test cylinders. Rebound numbers are correlated to compressive strength in units of MPa. The GROW and control materials produced the same correlation curves.	47
3.7 Rubber washers were made of 1/8" thick commercial grade Rubber-Cal Neoprene and were stamped with 2" and 1" diameter leather punches. The labeling of disc identification codes is visible on the top row of rubber washers.	49
3.8 Each disc was fitted with 1" nominal PVC pipe through the center hole to prevent damage to the disc via abrasion from the chain.	50
3.9 Five discs were strung onto each chain segment and fixed in place along the chain with a piece of threaded rod bolted into the exposed chain link above and below the disc.	51
3.10 Rubber washers provide protection against abrasion from the threaded rod and nuts. The threaded rod and nuts secure each disc's location on the chain.	51
3.11 The small forklift used to lower and lift hanging research structures from the pier into the water. A 130-lb counterweight was used to balance the forklift.	52
3.12 Side-view of the flume. The test section is 3 m long. The plate securely holds the calcium-ion selective electrode with the electrode tip 5 cm downstream from the discs and 3.5 cm from the water surface. The water velocity was 10 cm/s. The water depth was 7 cm, which provided 1cm of water flow above the discs. From the side-view there appears to be three discs, but there are five discs on the bed of the flume.	55
4.1 GROW research discs retrieved from Fallon Pier. Left-to-right: 90-day, 180-day, 330-day, 420-day retrievals on November 14 <sup>th</sup> , 2019, February 12 <sup>th</sup> , 2019, July 13 <sup>th</sup> , 2020, and October 6 <sup>th</sup> , 2020 respectively.	60
Figure 4.2. Percent cover of benthic functional groups for every disc deployed.	66
4.3 A disc from treatment group 420G that has been dehydrated to reveal only calcareous recruitment. The top surface of this disc from treatment group 420G is almost entirely colonized by barnacles.	67

4.4 On the left is a dehydrated disc from treatment group 420G, on the right is a dehydrated disc from treatment group 180G. Barnacle percent coverage on the innermost surface increased with submersion time.	67
4.5 nMDS plot for eight multivariate objects (eight treatment groups). Points represent treatment groups. Treatments groups that are more similar to one another are ordinated closer together. The axes and orientation are arbitrary. Treatment groups 330C and 330G are highly similar to each other, as are treatment groups 420C and 420G.	69
4.6 Calibration curve of the calcium ion selective electrode. The electrode takes measurements in millivolts, which has a log-linear relationship with concentration in ppm. The low concentration calibration solution (10 ppm), high concentration calibration solution (1000 ppm), tap water, and aquarium concentrations are mapped on the calibration curve for comparison.	72
4.7 Plot of calcium ion concentration (ppm) against time (min) for 5 GROW discs that were subjected to three continuous runs in the flume at 10 cm/s water velocity. The instrument uncertainty is < 1 ppm Ca <sup>2+</sup> .	74
4.8 Plot of calcium ion concentration (ppm) against time (min) for 5 control discs that were subjected to three continuous runs in the flume at 10 cm/s water velocity. The instrument uncertainty is < 1 ppm Ca <sup>2+</sup> .	75
4.9 Average compressive strength (MPa) of GROW and control discs before field treatment and after 90, 180, 330, and 420 days of submersion in the field. Standard deviation is represented by the error bars. Compressive strength data represented here is from rebound hammer testing, although Instron™ compressive strength testing was also conducted to validate rebound hammer measurements. The minimum compressive strength required of marine concrete is 35 MPa as designated by the American Concrete Institute; the industry standard minimum is represented via a gray horizontal line.	80

## List of Tables

3.1 40 discs were deployed at Fallon Pier the on August 12 <sup>th</sup> , 2019, 20 of which were control formula discs, and 20 of which were GROW formula discs. A subset of discs remained in the field for 90, 180, 330, or 420 days.	42
--	----

The original treatment design called for disc removal after 3, 6, 9, or 12 months with consistent 90-day time intervals, but the COVID-19 pandemic delayed the retrieval of the third and fourth sets of discs.

3.2 The Fallon Pier experiment included eight field treatments for 40 discs. The 40 discs were hung from the pier with 8 chains, with 5 discs per chain. Each chain was referred to as a research structure. This table describes which discs were hung on each research structure, and which treatment group each research structure belonged to.	43
4.1 List of organisms observed on the five discs of each treatment group. Bolded headers indicate which treatment group the column represents.	61
4.2 Photographs of observed organisms on retrieved discs. Photos captured with an iPhone 11 camera without magnification ( <i>Didemnum</i> sp., <i>Asciella aspersa</i> , <i>Botrylloides violaceous</i> , kelp, mussels, <i>Styela clava</i> , European green crab, common slipper shell) or with 10x magnification (Hydroid, barnacle, tubes, algae).	62
4.3 Abbreviations for functional group and species names. The species and functional group names were abbreviated for plotting purposes, and the abbreviations are listed below in the second column. The common name is included in the third column for reference.	63
4.4 Average percent cover of the surface, organized by treatment group. Each treatment group had five deployed discs. The surface of each disc was sampled at 100 points. The average percent cover was calculated by summing data over 500 total points and dividing by 5 discs to produce percent cover equaling 100 in this table. Species names have been abbreviated according to Table 4.3. The first number reported is the average percent cover, and the number in brackets is the standard deviation.	65
4.5 Average percent cover of calcareous recruitment on concrete surface as observed after disc dehydration and removal of all non-calcareous growth. Three out of five discs from each of the eight treatment groups was tested with the rebound hammer because of the labor-intensive surface preparation process.	68
4.6 Counts and sizes of mussels observed on discs retrieved from the 330-day and 420-day submersion group.	68
4.7 SIMPER analysis compared similarity in species composition between treatments with the same submersion time but different material. SIMPER calculates average similarity as a percentage, and also the % contribution	70



to the dissimilarity by species. Take the comparison of 90C and 90G as an example: these two treatment groups had an average similarity in species composition of 81.52%, with barnacles contributing to 21.15% of the dissimilarity between the two treatment groups.

4.8 SIMPER analysis data for comparing similarity in species composition between treatments with different submersion times regardless of material. 70

4.9 Calcium ion concentration was measured for 24 hours of submersion and 72 hours of submersion for single discs of control and GROW material in still water 7" x 7" x 6" aquariums. 71

4.10 Compressive strength of 3"x 6" test cylinders and untreated discs as measured by an Instron™ compression machine. Test cylinders and untreated discs were loaded in compression at a rate of 0.2 MPa/s. Five test cylinders of each material were tested, and three discs of each material were tested. The average is the first number reported and the standard deviation is reported in brackets. The p-values are reported for independent paired t-tests performed between material types and between test cylinders vs. discs. 78

4.11 Compressive strength of discs before field deployment as measured by a rebound hammer. Three test cylinders were tested. All forty field discs were tested prior to deployment. The average is the first number reported and the standard deviation is reported in brackets. The p-values are reported for independent paired t-tests performed between material types and between test cylinders vs. discs. 78

4.12 Compressive strength of discs after field deployment as measured by a rebound hammer. Three discs from each treatment group were tested. The three discs furthest from the bed in each treatment group was selected to avoid interference from the effect of depth. The average is the first number reported and the standard deviation is reported in brackets. The p-values are reported for independent paired t-tests performed between material types. 79

4.13 Compressive strength of discs after field deployment as measured by an Instron compression machine. Discs were dehydrated in a 200° C dehydration oven, then were loaded in compression at a rate of 0.2 MPa/s. One disc from each treatment group was tested. The disc furthest from the bed in each treatment group was selected to avoid interference from the effect of depth. 79



# Chapter 1

## Introduction

### 1.1 Motivation

More than 60% of the world's largest cities are located within 100 km of the coast, and coastal cities are projected to continue growing in population size (Barragan and de Andres 2015; Tibbetts 2002). Coastal landscapes continue to be altered on a global scale by man-made infrastructure designed to facilitate urbanization in response to population growth in coastal cities, and to protect coastal communities from sea level rise and increasing storm intensities (Bishop et al. 2017). Coastal and marine infrastructure, such as seawalls, breakwaters, piers, dykes, and pontoons, have replaced natural intertidal, subtidal, and benthic habitats along many coastlines (Perkol-Finkel and Sella 2014). In the Boston Harbor Islands National Recreation Area, concrete seawalls have replaced some of the mussel reefs, salt marshes, mixed coarse substrates, and rocky substrata that comprise the natural coastline (Bell et al. 2005).

Coastal infrastructure has a multitude of impacts on biodiversity and ecosystem functioning (Chapman 2003; Perkol-Finkel and Sella 2014). Studies on the impacts of man-made coastal infrastructure have focused on whether they alter the ecology of the environments in which they are constructed (Chapman 2003; Perkol-Finkel and Sella 2014), and whether they can act as successful replacements to the habitats provided by

natural intertidal, subtidal, and benthic reefs, marshes, and rocky shores (Waltham and Sheaves 2018; Perkol-Finkel and Sella 2014). Man-made coastal infrastructure differs from natural habitats physically in terms of surface complexity, surface area, orientation, and material strength, and chemically in terms of material composition and potential for chemical leaching into surrounding waters (Chapman and Browne 2014; Chapman 2003; Perkol-Finkel and Sella 2014). The habitat provided by man-made coastal infrastructure typically supports ecological communities that are significantly different from ecological communities on natural habitats. The communities supported by man-made infrastructure are often characterized by greater abundances of invasive species and aquatic nuisance species, and lower overall biodiversity (Kennedy et al. 2020; Firth et al. 2014).

Biodiversity in coastal environments plays an important role in maintaining the functionality and productivity of ecosystems, the resiliency of ecological habitats and communities against environmental threats, and the ecosystem services provided to humans (Rees et al. 2018). Functional and productive coastal ecosystems provide a number of important services, including water quality maintenance, reduction in shoreline erosion, creation of feeding and nesting habitats for other marine species, and increased opportunity for recreational fishing or shellfish harvesting (Barbier et al. 2011). These ecosystem services are not only ecologically important, but also economically important. Estimates of the value of ecosystem services provided by biodiverse coastal ecosystems are typically upwards of \$5500 USD per hectare (Barbier et al. 2011; Grabowski et al. 2012). Biodiverse ecosystems are also better equipped to face the threat of invasive species, which often impair the recreational, commercial, and agricultural uses of coastal waters because of their tendency to outcompete native species and foul surfaces of infrastructure and watercraft (EPA 2020a).

In the last 15 to 20 years, new approaches have emerged in the design of coastal infrastructure, which utilize green infrastructure design principles to mitigate the

impacts of man-made coastal infrastructure (eg. Perkol-Finkel and Sella 2014; Firth et al. 2014). Green infrastructure uses and/or mimics natural ecosystems to provide infrastructure functions, while also providing benefits to the surrounding environment (EPA 2020b). With regard to seawalls and breakwaters, recent green infrastructure designs have focused on incorporating physical features of natural habitats such as complex surface texture, water-retaining features, and increased intertidal area, in order to attract biodiverse marine communities (Chapman and Browne 2014; Waltham and Sheaves 2018; Loke 2015; Firth et al. 2014). A limited number of projects have investigated chemically altering the concrete used to construct seawalls to make them more hospitable to marine organisms. A 2014 study that reformulated marine concrete to have reduced alkalinity while increasing concrete surface complexity found that these design changes increased the recruitment of native species and water-filtering species (Perkol-Finkel and Sella 2014). A 2018 study incorporated ground oyster shells in the concrete formula and compared the formula change with different surface textures, orientations, and submersion times on biodiverse recruitment, and found that the inclusion of ground oyster shells increased recruitment of mollusk species, but did not have as much of an effect on community structure as texture and orientation (Hanlon et al. 2018). Mollusk species are considered desirable in many marine environments because of their water-filtering capabilities and because they have been shown to improve the material strength of submerged concrete (Risinger 2012). There is currently limited knowledge on concrete formula enhancement and its potential influence on 1) material strength and 2) marine recruitment of biodiverse assemblages and mollusks as a target species, despite the importance of this topic to the development of green coastal infrastructure design practices.

## **1.2 Project Overview**

The primary objective of this study was to compare the performance of reef mimics constructed from marine concrete with those constructed with CaCO<sub>3</sub>-enriched concrete

with regard to recruitment and durability, and to evaluate correlations with seasonal influences over a one-year period. The main objective was to improve our understanding of the suitability for CaCO<sub>3</sub>-enriched concrete in improving the biodiversity and durability of seawalls constructed in New England, in order to better inform green seawall design choices.

Textured reef mimics in both standard marine concrete and CaCO<sub>3</sub>-enriched concrete were constructed and deployed along the coast in Dorchester Bay, Massachusetts. Reef mimics were divided into four groups exposed to different durations of field exposure. All four groups were deployed together at the start, but removed at different times throughout the year. The reef mimics were studied post-deployment to assess species recruitment and changes in material strength. Reef mimics were also studied in a flume to observe leaching of CaCO<sub>3</sub> in still and moving waters to assess the potential of this concrete formula and geometry to leach Ca<sup>2+</sup> and CO<sub>3</sub><sup>2-</sup> ions as a recruitment cue, and as building blocks for shell precipitation.

# Chapter 2

## Background

### **2.1 Seawalls versus natural intertidal, subtidal, and benthic habitats**

Concrete seawalls differ from natural intertidal, subtidal, and benthic habitats in a number of fundamental ways. One of the most prominent differences is the slope and intertidal area of the habitat surface: natural rocky substrata or reefs tend to slope downwards into the water, whereas seawalls are typically vertical walls, which creates less surface area in the intertidal zone, relative to the natural sloped landscape.

Intertidal species that were previously distributed across a larger surface area are now constrained and superimposed on the seawall; this change in the amount of space available to species can alter not only their distribution but also their competitive interactions and community dynamics (Waltham and Sheaves 2018). Reduced area and ecological niches are particularly disadvantageous for specialist species, species that require specific resources to grow and survive. This might explain why seawalls are usually characterized by a small number of generalist species. Another difference between both habitats is surface complexity: seawalls have a smooth surface that lacks the complexity of natural habitats. Surface complexity on natural habitats consists of cracks, crevices, pits, and other textured or water-retaining features. These surface

features support wider ranges of species because they increase surface area, provide pockets of quiescent waters, entrap nutrients, and expand the range of environments available to organisms looking for shelter or substrate (Chapman and Browne 2014). Chemically, marine concrete is highly alkaline with a pH of 12 to 14 (Mehta 1986). Many species are not able to withstand the alkalinity on the surface of a newly submerged concrete structure, which negatively impacts early-stage recruitment (Perkol-Finkel and Sella 2014; Hanlon et al. 2018). All of these factors contribute to a seawall ecosystem which lacks species diversity (Chapman et al. 2009).

## **2.2 Mollusk species as ecosystem engineers and concrete fortifiers**

Mollusks are aquatic invertebrates with soft unsegmented bodies and external calcareous shells, although a few exceptional mollusk species do not have shells (Marin and Luquet 2004). In many coastal habitats, mollusks serve as ecosystem engineers: a species that plays a significant role in creating, modifying, and maintaining habitat. The shells of mollusks in aquatic ecosystems serve as substrate for the attachment of microbes and marine invertebrate larvae, provide protection from predators or harsh environmental conditions, and control the transport of nutrients and sediments in the habitat. Because of the ecosystem engineering role mollusks play in the habitats they populate, they exert significant influence on community structure and thus biodiversity (Gutiérrez et al. 2003).

When mollusks populate the surface of a substrate, their hard, impermeable shells are able to protect the substrate from material degradation due to impacts from wave energies and from other species that burrow and damage substrate surfaces. Concrete cylinders that were populated by adult oysters over a two-year period demonstrated significantly higher material flexural strengths when tested against to bare concrete cylinders (Risinger 2012). Their potential as ecosystem engineers and concrete fortifiers make mollusks desirable as a target recruit to green seawalls.



## **2.3 Standard marine concrete: physical and chemical properties, material strength and durability, and calcium ion leaching potential**

Standard marine concrete typically has a pH of 12 to 14. The main ingredients of standard marine concrete are aggregates (sand, gravel, or crushed stone) and cement paste. Cement paste is formed when cement is mixed with water, resulting in hydrolysis reactions and paste formation (Mehta 1986).

Marine concrete is designed with a lower permeability to protect the concrete from degradation, as discussed below. The American Concrete Institute has standards on concrete construction, which dictate water-cement ratio, cement content, cement type, pozzolans, and aggregates. The industry standard for testing concrete strength is a 28-day cylindrical compressive strength test, in which concrete is allowed to cure for 28 days before being subjected to uniaxial compressive load until failure. Marine concrete must satisfy a 35 MPa load minimum to be used in the construction of seawalls or other coastal infrastructure (Suprenant 1991).

Marine concrete is typically categorized into three exposure zones: submerged, splashed, and atmospheric. Concrete in the submerged zone is always underwater, concrete in the splashed zone is exposed to continuous wetting and drying, and concrete in the atmospheric zone is mostly exposed to air. Concrete in the splashed and atmospheric zones are the most vulnerable to degradation from exposure to seawater (Suprenant 1991). The main pathways for concrete degradation in the presence of heavy seawater exposure include: sulfate attack, calcium hydroxide (lime) leaching, alkali-aggregate expansion, salt crystallization, freeze-thaw, erosion and abrasion from wave energy (Lagerblad 2007). Our discussion will focus on calcium hydroxide leaching because of the relevance of calcium as a recruitment cue.

Calcium leaching is inevitable whenever concrete is in contact with water. The most commonly used cement paste is Portland cement, which contains calcium as roughly 30% of its solid mass. Standard marine concrete typically has a pH of 12 to 14, and seawater typically has a pH of 8.1. This difference in pH leads to the dissolution of ions off the concrete surface, calcium being one of the main ions. Water that enters the pores in the concrete structure also dissolves calcium ions, and a concentration gradient is formed between the calcium-ion rich pore solution and external seawater, which leads to diffusion of calcium away from the concrete (Tan et al. 2017; Heukamp 2003).

The porosity of marine concrete influences calcium leaching and the durability of the concrete. The two primary types of pores in marine concrete are capillary pores, which have a characteristic size in the micrometer range, and macropores, which have a characteristic size in the millimeter range. Within capillary pores, Portlandite ( $\text{Ca}(\text{OH})_2$ ), a hydrolysis product from the reaction of water and Portland cement, dissolves first, before any other hydrolysis products. Portlandite has a crystal structure that allows it to dissolve completely in water, thus when water enters capillary pores, the space originally occupied by Portlandite is converted to porosity. Dissolution of Portlandite can increase the total porosity of a submerged concrete structure by 10% to 15% (Heukamp 2003).

Calcium leaching has a direct effect on the material strength and durability of a concrete structure. A cement paste that has leached enough calcium for the surrounding waters to reach a steady-state concentration has a compressive strength 10% of the pre-leaching value (Carde et al. 1996).

There exists a paradox with regard to green seawall design: calcium leaching from standard marine concrete might recruit bivalve species, but also reduces the compressive strength of the concrete and makes concrete more porous and thus susceptible to future degradation and further reduction in compressive strength. Moreover, despite heavy

leaching of calcium from standard marine concrete, carbonate ions, the other important ion in bivalve shell formation, are not supplied, and the high alkalinity is still damaging to many marine species. Thus, exploration of marine concrete formula improvements is worthwhile.

## **2.4 Intertidal, subtidal, and benthic marine habitats and species of Boston Harbor Islands national park area**

The Boston Harbor Islands national park area is comprised of 34 islands in Massachusetts Bay, the same bay where my field experiment was conducted. The 34 islands provide important habitat to intertidal and benthic species in Massachusetts Bay. The Boston Harbor Islands features a wide range of diverse habitats, including salt marshes, mudflats, and bedrock outcrops. The two islands closest to the mainland, Thompson Island and Worlds End, have the highest percentage of peat and fine sediments, and the best-developed salt marshes. Middle and inner islands like Georges, Gallops, and Lovells Islands have mainly mixed coarse substrate and large mussel reefs. Middle to outer islands, Langlee and Raccoon, have much higher percentages of rocky substrata. The two outer, more exposed islands, Outer and Little Brewster, are dominated by rocky substrata such as bedrock and boulders (Bell et al. 2005).



Figure 2.1: Map of the Boston Harbor Islands national park area with the ten largest islands labelled by name, and with the field site marked in red. Boston Harbor Islands national park area is comprised of 34 total islands in Massachusetts Bay, the same bay in which our field site was located.

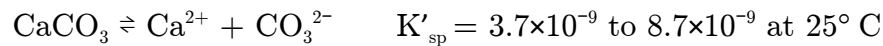
Biotic assemblages present on the Boston Harbor Islands include (in order of greatest percent area): *Mytilus* reef (salt water mussels), *Spartina alterniflora* (saltmarsh cordgrass), mixed brown algae, *Ascophyllum* (rockweed), green algae, *Spartina patens* (saltmeadow cordgrass), red algae, *Phragmites* (common reed), and *Salicornia* (salt tolerant flowering plants) (Bell et al. 2005). A 2001 species survey of the Boston Harbor Islands and Boston Harbor found 95 species of animals, 70 species of marine algae, and 15 species of vascular plants. Amongst the animal phyla recorded, Annelida, Arthropoda, Mollusca, and Bryozoa had the highest number of species. Amongst the animal classes recorded, Crustacea, Polychaeta, and Gastropoda had the highest number of species (Bell et al. 2005).

Of the 95 animal species, 11 were invasive. Of the 70 marine algae species, 4 were invasive. Non-native invaders commonly observed during the 2001 survey included the ascidians, *Botrylloides violaceous* (Pacific colonial sea squirt), *Styela clava* (Pacific rough sea squirt), and *Botryllus schlosserei* (golden star tunicate). *B. violaceous* was one of the most common encrusting marine organisms in the lower intertidal range, often

outcompeting barnacles and seaweeds. *S. clava* was very common in Boston Harbor and was found on almost all hard substrates, including on mussel assemblages. *B. schlosserei* was found mainly on hard substrates but was not observed as frequently as the other ascidians. The Asian shore crab, *Hemigrapsus sanguineus*, was not observed on the Islands but was observed in Boston Harbor (Bell et al. 2005; Osman and Whitlatch 1999).

## 2.5 The calcium carbonate dissolution-precipitation reaction

In our study, the calcium carbonate dissolution-precipitation reaction is relevant to 1) precipitation of mollusk shells and 2) the dissolution from concrete structures and subsequent diffusion of  $\text{Ca}^{2+}$  and  $\text{CO}_3^{2-}$  ions. The equilibrium of calcium carbonate precipitation and dissolution is described by the following equation:



The solubility product  $K_{\text{sp}}$  is defined as the product of the concentration of calcium ions and carbonate ions ( $[\text{Ca}^{2+}] \times [\text{CO}_3^{2-}]$ ). If the solubility product  $K_{\text{sp}}$  is less than the equilibrium constant solubility product  $K'_{\text{sp}}$ , no calcium carbonate can be precipitated, and the growth of hard-shelled organisms will be limited.  $K'_{\text{sp}}$  is dependent on temperature, salinity, pressure, and the carbonate mineral phase. Calcium carbonate is a common additive in oyster-promoting concrete mixes because it increases  $[\text{Ca}^{2+}]$  and  $[\text{CO}_3^{2-}]$  in surrounding waters in order to promote the recruitment of hard-shelled organisms and to enhance the availability of shell-building ions.

The two most common calcium carbonate mineral phases are aragonite and calcite. Aragonite and calcite have the same chemical formula,  $\text{CaCO}_3$ , but differ in crystal

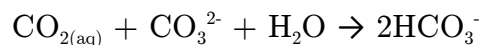
structure. Aragonite is the crystal form that usually forms when calcium carbonate precipitates into shells in seawater. The aragonite saturation state  $\Omega_{aragonite}$  is a measure of the thermodynamic tendency of aragonite to precipitate or dissolve.  $\Omega_{aragonite}$  is a function of calcium and carbonate ion concentrations as well as the equilibrium constant solubility product:

$$\Omega_{aragonite} = \frac{[Ca^{2+}] [CO_3^{2-}]}{K'_{sp}}$$

When  $\Omega_{aragonite}=1$ , seawater is in equilibrium with respect to aragonite. When  $\Omega > 1$ , seawater is supersaturated with respect to aragonite, and aragonite will precipitate. When  $\Omega < 1$ , seawater is undersaturated with respect to aragonite, which results in dissolution of existing aragonite minerals (eg. Green et al. 2013).

## 2.6 Impact of increasing atmospheric CO<sub>2</sub> on shelled organisms

The global average atmospheric carbon dioxide (CO<sub>2</sub>) level was approximately 400 ppm in 2019. The last time atmospheric CO<sub>2</sub> was this high was more than 3 million years ago. Atmospheric CO<sub>2</sub> levels have been steadily increasing mainly due to fossil fuel use and deforestation (Lindsey 2020). Since atmospheric CO<sub>2</sub> and aqueous CO<sub>2</sub> in oceans must remain in equilibrium, increasing CO<sub>2</sub> levels in the atmosphere have impacts on carbonate speciation and pH in the global oceans. When CO<sub>2</sub> dissolves in water to produce aqueous CO<sub>2</sub> (CO<sub>2(aq)</sub>), it rapidly reacts with water to form carbonic acid (H<sub>2</sub>CO<sub>3</sub><sup>\*</sup>). Carbonic acid disassociates into bicarbonate ions (HCO<sub>3</sub><sup>-</sup>) and protons (H<sup>+</sup>). Bicarbonate ions disassociate into carbonate ions (CO<sub>3</sub><sup>2-</sup>) and protons. The increase in protons due to increased CO<sub>2</sub> levels decreases the pH of ocean water, a process that is referred to as ocean acidification. However, seawater has the ability to provide natural buffering via:



Bicarbonate goes on to partially dissociate, releasing protons and increasing ocean acidity, but the pH effects are smaller in this buffered system. Dissolved organic carbon (DIC) is defined as the sum of the concentrations of carbonate species products  $[\text{CO}_{2(\text{aq})}] + [\text{HCO}_3^-] + [\text{CO}_3^{2-}]$ . The distribution of DIC between these three species depends on pH. Today's oceans typically have a surface pH of 8.1, thus bicarbonate is the dominant species. As ocean pH lowers,  $[\text{CO}_{2(\text{aq})}]$  and  $[\text{HCO}_3^-]$  will increase as  $[\text{CO}_3^{2-}]$  decreases, putting shelled organisms who rely on  $\text{CO}_3^{2-}$  at risk for dissolution and reduced growth (Barker and Ridgwell 2012).

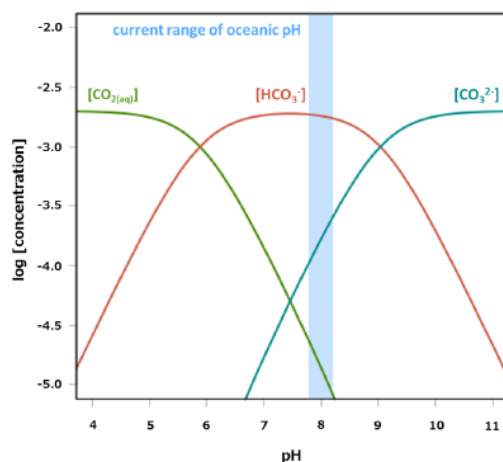


Figure 2.2: Concentrations of the three dissolved inorganic carbon species are dependent on pH. As ocean acidification progresses, oceanic pH decreases, and the concentration of carbonate ion decreases, putting shelled organisms who rely on calcium and carbonate ions at risk.

## 2.7 Calcium carbonate precipitation in mollusk shells

Mollusks, such as oysters and mussels, are soft-bodied marine organisms that develop external calcified structures for support and protection. Calcium carbonate accounts for 95 to 99% of a typical mollusk shell by weight. The remaining 1 to 5% is made up of anatomical components that help mollusks to precipitate calcium carbonate to grow and maintain their protective shells. These anatomical components are able to drive the calcium carbonate dissolution reaction forward to make ions readily available for shell

precipitation, without dissolving the existing mollusk shell into ions (Marin and Luquet 2004).

Mollusk shells have a unique protein outer layer, called the periostracum. Mollusks secrete periostracin protein, which undergoes a biochemical process to become a highly insoluble outer layer. The periostracum seals the inner compartments of the mollusk, allowing the mollusk to pump ions from the external environment into its body to create supersaturated calcium and carbonate ion solutions, which then precipitate to form aragonite layers of shell beneath the periostracum layer (Waldbusser et al. 2011).

## **2.8 Factors influencing biodiverse recruitment: chemical cues, biofilms, flow conditions, substrate surface topography**

Successful recruitment of diverse communities onto surfaces of coastal infrastructure requires successful settlement of planktonic larvae. For most marine invertebrate species, settlement marks a point of transition in their life cycles from a planktonic larval phase to a sessile adult phase (Pawlik 1992). Settlement rates and distributions of marine larvae are important factors in determining population dynamics and community structure in intertidal and benthic environments (Browne and Zimmer 2001). Recent studies have suggested that the larval settlement process is a dynamic and multi-variable process whereby larvae actively respond to a wide range of cues and environmental parameters to select a site that optimizes conditions for attachment, growth, and survival (Green et al. 2013; Vasquez et al. 2013; Browne and Zimmer 2001). We discuss previous work on factors that influence marine invertebrate larval settlement: chemical cues, flow conditions, and substrate surface complexity.

Chemical cues regulate many critical aspects of marine organism behavior, including predator-prey interactions, transfer of energy and nutrients within and among ecosystems, and settlement and attachment onto substrate surfaces (Hay 2009).



Chemical cues emitted from mollusk reefs, crushed shells, and biofilms increase settlement of various marine invertebrate species to substrate surfaces (Hay 2009; Vasquez et al. 2013).

In oyster hatcheries and farms across New England, crushed mollusk shells have been used as a substrate or substrate enhancer since colonial times (Lackovic 2019; Boyle 2020). Crushed shells prepared from the shells of oysters, mussels, clams, and scallops provide a substrate that attracts oyster larvae and encourages attachment and colonization. Factors that influence the success of crushed shells as a settlement cue for oysters include the amount of crushed shells provided and whether the type of crushed shell is of the same species as the target recruit species. Laboratory and field studies of *Crassostrea gigas* (Pacific Oyster) larvae have found that larval settlement is proportionate to the amount of crushed shell chips provided to larvae, regardless of shell species (Vasquez et al. 2013; Hay 2009). Larvae of *C. gigas* and *Crassostrea virginica* (Eastern Oyster), when given the option of shells of their own species (conspecific shells) and shells of other mollusk species (heterospecific shells), display greater settlement on conspecific shells (Vasquez et al. 2013; Crisp 1967; Pawlik 1992). Crushed shells are successful in recruiting mollusks not only as pure crushed shell substrates, but also as an ingredient in concrete mixes. The inclusion of crushed oyster shells as an ingredient in concrete mix significantly increased mollusk recruitment in several field studies (Hanlon et al. 2018; Vasquez et al. 2013; Hay 2009).

The chemical basis of the settlement cue released from mollusk shells is an insoluble glycoprotein which lines the outer and inner surfaces of mollusk shells. In studies in which the outer and inner surface layers of mollusk shells were removed, shells did poorly at recruiting larvae (Crisp 1967; Vasquez et al. 2013). The outermost layer of most mollusk shells is made up of a thin organic coating called the periostracum, and the inner layer is typically an organic-inorganic layer of composite material called nacre, also known as mother of pearl (Marin and Luquet 2004). Although the exact

glycoprotein cue has not been identified from mollusk shells, peptide (small protein) analogues have been synthesized and used as a cue to induce settlement of larvae in both field and lab studies. The synthetic peptide analog glycyl-glycyl-L-arginine (GGR) has successfully induced settlement of both oyster and barnacle larvae (Browne and Zimmer 2001; Turner et al. 1994).

Larvae have been demonstrated to respond to chemical cues in the cm-mm range of the water column above a cue-emitting substrate, not just to surface-adsorbed chemical cues (Gross, Werner, and Eckman 1992; Turner et al. 1994; Browne and Zimmer 2001). Marine larvae typically have weak swimming abilities relative to the horizontal flows present in benthic and intertidal environments, with reported swim speeds of only 1 mm/s horizontally and 3.14 mm/s vertically. However, marine larvae are able to significantly increase their swimming speeds downwards in response to a chemical cue emitted from the bed, even in the presence of currents (Turner et al. 1994; Gross, Werner, and Eckman 1992). In currents of 2 to 6 cm/s, oyster larvae 7 cm above GGR-emitting substrate were able to swim rapidly downwards, demonstrating increased settling for cue-emitting substrates versus no-cue substrates (Turner et al. 1994).

In addition to glycoproteins from mollusk shells, calcium and carbonate ions themselves can provide chemical cues that facilitate larvae settlement. Aragonite saturation state  $\Omega_{aragonite}$  is a measure of the thermodynamic tendency of aragonite to precipitate or dissolve based on calcium and carbonate ion concentrations, as well as temperature, salinity, and oxygen saturation. Higher  $\Omega_{aragonite}$  has been shown to increase settlement of *Mercenaria mercenaria* (hard clam) larvae.

Biofilms are thin layers of accumulated micro-organisms that colonize surfaces of submerged coastal structures. Biofilms not only coat substrate surfaces, but can also coat other colonizing species that attach to substrates. They contribute to nutrient turnover and productivity within marine communities and induce settlement of marine

larvae (Hay 2009). Larvae of certain species can differentiate between biofilms of varying compositions, densities, and ages, and adjust their settlement response based on biofilm differences. Larval responses to biofilms can either be facilitatory (encourages settlement), or inhibitory (discourages settlement) (Wieczorek and Todd 1998).

*Alteromonas colwelliana* bacteria have been shown to settle on oyster shells of both alive and dead oysters, creating a biofilm that increases settlement of oyster larvae. Flow regime and surface shear stress are important determinants of accumulation rates and microbial community structure of biofilms (Lau and Liu 1993; Neal and Yule 1994). Shear stress acts tangential to the settlement surface, and in combination with drag and lift forces, can cause settling larvae to be dislodged from the surface back into the flow. Biofilm biomass accumulation is significantly reduced on horizontal planar surfaces experiencing high shear stress (Lau and Liu 1993). On cylindrical or corrugated surfaces, the velocity spatial gradients drive preferential accumulation to the leeward side of cylinders and in the crevices in between raised ridges (Secchi et al. 2020). The differences in microbial community structure that arise from varying flow conditions can drive differences in recruitment of marine larvae. For example, the larvae of the barnacle species *Elminius modestus* and *Balanus perforatus* can discriminate between bacterial films characteristic of certain hydrodynamic environments in the laboratory (Neal and Yule 1994).

The flow regimes of benthic and intertidal environments also influence marine larval recruitment in addition to biofilm accumulation. Local hydrodynamics determine whether larvae will attach to substrate, but even after contact is made with the substrate, larvae can release themselves back into the flow if the first site was hydrodynamically unsuitable (Whitman and Reidenbach 2012). When larvae land on substrate surfaces, they must experience sufficiently low shear stress over a period of time in order to successfully attach. A study on barnacles demonstrated that higher velocity lead to increased barnacle larvae populations due to higher arrival rates, but

barnacle larvae often selected local low shear areas on the substrate for attachment (Mullineaux and Butman 1991).

Local hydrodynamics have proven to be an important factor in oyster reefs as well. Well-developed oyster reefs have higher rates of recruitment when compared to oyster restoration sites and mud flats, because reefs typically have many more interstitial spaces and pockets between oysters of varying sizes and between layers of oysters. Interstitial areas between or under oysters provide pockets in which velocity and turbulence are reduced (Whitman and Reidenbach 2012). Oysters within reef interstices grow faster and live longer than oysters at the reef surface, suggesting that local hydrodynamics play an important role not only in recruitment of larvae but also in the health and survival of adults (Bartol, Mann, and Luckenbach 1999).

Pockets in the surfaces of intertidal and benthic substrates not only provide relief from high velocity and turbulence to settling larvae and growing adults, but also provide micro-habitats that support biodiverse recruitment. The positive relationship between surface complexity and biodiversity is well-studied (Loke 2015; Chapman 2003; Chapman and Browne 2014; Firth et al. 2014). Natural intertidal and benthic environments have water-retaining features, such as pits, crevices, and tide pools, which increase surface area, provide pockets of quiescent waters, entrap nutrients, and expand the range of environments available to organisms looking for shelter or substrate (Chapman and Browne 2014). Increased surface complexity provides micro-habitats by expanding the range of environments available to organisms: exposure to light, temperature, salinity, and oxygen can vary across a surface with different 3-dimensional features (Loke 2015). Different species have different preferences for environmental conditions, thus more complex surfaces are better able to facilitate the recruitment of biodiverse marine assemblages. Surfaces with features of varied sizes are also important in supporting biodiverse recruitment, in addition to supporting healthy growth of larvae into adults. Surface features on the mm scale provide ideal settlement, nesting, and

feeding habitats for larval-stage recruits and smaller organism like barnacles (Perkol-Finkel and Sella 2014; Loke 2015). Surface features on the cm scale provide ideal spaces for larval-stage recruits to grow into adults while hiding from predators (Airoldi 2003).

## 2.9 Calcium carbonate dissolution from a concrete plate

At the scale of the artificial research structures used in this thesis study (10 cm diameter, 6.4 cm height cylinders), the hydrodynamic response effecting biological recruitment and calcium leaching is dominated by boundary-layer formation on the concrete surface. As a reference for discussion, the boundary layer formed of a flat concrete plate can be used to model.

A boundary layer is a thin layer of viscous fluid close to the solid surface of the concrete plate that forms at the leading edge ( $x=0$ ) as fluid flows over the plate. The thickness of the viscous boundary layer is represented by  $\delta$ . The viscous boundary grows in thickness in the direction of fluid flow,  $\delta(x) = 5 \sqrt{\frac{\nu x}{U}}$ , in which  $U$  is the mean velocity and  $\nu$  is the kinematic viscosity (White 2008). As the viscous boundary layer becomes thicker, it is effected by roughness on the concrete surface or turbulent oscillations in the outer flow, and can transition into a turbulent boundary layer. The transition typically occurs when the Reynolds number  $R_x = \frac{Ux}{\nu} \approx 10^5$ , but this can vary depending on surface roughness of the plate (White 2008). When the boundary layer becomes turbulent, the viscous boundary layer becomes a thin layer close to the plate surface, and is now called the viscous sublayer. The thickness of the viscous sublayer depends on the friction velocity  $u_{b*}$  on the plate surface:  $\delta_s = 5 \frac{\nu}{u_{b*}}$  to  $10 \frac{\nu}{u_{b*}}$ . Within the viscous sublayer, there exists an even thinner layer, the diffusive sublayer, in which ion transport perpendicular to the concrete surface only happens through molecular diffusion. The thickness of the diffusive sublayer is  $\delta_c = \delta_s Sc^{1/3}$ , in which  $Sc$  is the Schmidt number  $Sc = \frac{\nu}{D_m}$ . The molecular

diffusivity of calcium ions in water is  $D_m = 1.312 * 10^{-9} \frac{m^2}{s}$  at 20° C (Ko et al. 2020

quoting Linder et al. 1976), and the kinematic viscosity of water is  $\nu = 10^{-6} \frac{m^2}{s}$  at 20° C,

thus  $\delta_c$  can be simplified to  $\delta_c = 0.09 \delta_s$ .

Fick's Law states that the rate of transfer of molecules by diffusion through a unit area is proportional to the concentration gradient (eg. Kays and Crawford 1993).

$$\text{Flux across } \delta_c = \dot{m} = -D_m A \frac{\partial C}{\partial z} = -D_m A \frac{C - C_{eq}}{\delta_c}$$

in which  $C$  is the concentration of the ion of interest, and  $C_{eq}$  is the equilibrium concentration of the ion in water. Mass conservation states:

$$\frac{\partial C}{\partial t} + u \frac{\partial C}{\partial x} + v \frac{\partial C}{\partial y} + w \frac{\partial C}{\partial z} = \frac{\partial}{\partial x} D_{m,x} \frac{\partial C}{\partial x} + \frac{\partial}{\partial y} D_{m,y} \frac{\partial C}{\partial y} + \frac{\partial}{\partial z} D_{m,z} \frac{\partial C}{\partial z} \pm S$$

in which  $S$  is the concentration of the ion at the source (the concrete boundary). In a system that is turbulent, well-mixed, and has no mean current, the terms

$u, v, w, \frac{\partial}{\partial x}, \frac{\partial}{\partial y}, \frac{\partial}{\partial z}$  reduce to zero, and the conservation of mass reduces to  $\frac{\partial C}{\partial t} = S$ .

Multiplying the system by volume ( $V$ ) allows for the source term  $S$  to be replaced by Fick's Law, giving:

$$\frac{\partial C}{\partial t} = - \left[ \frac{D_m A}{V \delta_c} \right] (C - C_{eq}) = -k(C - C_{eq})$$

in which  $k$  is a first-order rate constant,  $k = \left[ \frac{D_m A}{V \delta_c} \right]$ . With the initial condition

$C(t = 0) = 0$ , the ion concentration in the water due to the source at the bed is:

$$C = C_{eq}(1 - e^{-kt}).$$

When advection is present, the Peclet number must be considered. The Peclet number is the ratio of the rate of advection of molecules by the flow to the rate of diffusion or dispersion of the molecules driven by the concentration gradient.

Comparing advective transport against diffusive transport:

$$Pe_L = \frac{LU}{D_m} = Re_L Sc$$

Comparing advective transport against dispersive transport:

$$Pe_L = \frac{LU}{Kx}$$

in which  $Kx$  is the longitudinal dispersion coefficient, estimated to be  $Kx = 5.93u_{b*}h$  in which  $h$  is the height of the flow (Elder 1959). If  $Pe_L \gg 1$ , advective transport dominates, and thus diffusion or dispersion can be neglected. Steady-state concentrations can be calculated from mass conservation and the rate constant  $k =$

$$\left[ \frac{D_m A}{V \delta C} \right].$$

The transport of calcium ions from the surfaces of concrete substrates is relevant because of its influence on mollusk shell growth and recruitment of mollusk larvae via calcium as a chemical cue. Boundary-layer dynamics at the surfaces of concrete substrates is relevant because of its influence on benthic recruitment and community structure. Formulation of calcium carbonate-enriched concrete for coastal infrastructure design must have calcium carbonate content high enough to increase concentrations of calcium and carbonate ions in surrounding waters so that mollusks can utilize them for shell growth and maintenance. Depending on the flow conditions, the leaching of calcium and carbonate ions can occur either in a thin layer on the concrete surface,

called the diffusive sublayer, or ions can be carried downstream of a current and the concentration can be estimated at some streamwise distance away from the concrete.



# Chapter 3

## Methods

### 3.1 Experimental Methodology

#### 3.1.1 Artificial habitat structures

The artificial habitat structures used were constructed by Grow Oyster Reef LLC, a business based in Chesapeake Bay, Virginia that produces concrete reef-building products for recruiting oysters, improving water quality, and providing shoreline protection (Tickle, [www.growoysterreefs.com](http://www.growoysterreefs.com)).

The artificial habitat structures are discs with a 6.4 cm height, a 10 cm diameter, and a 3.2 cm diameter center hole. The center hole facilitates deployment by allowing discs to be strung onto ropes, chains, or pipes. Numerous studies have demonstrated that surface complexity facilitates recruitment of diverse benthic assemblages (Chapman and Browne 2014; Waltham and Sheaves 2018), thus the lateral surfaces of the discs are textured with two rows of evenly spaced hemispherical cavities that are 2.0 cm in diameter, 0.6 cm in depth from the lateral surface, and 0.5 cm apart. The inner surfaces of each hemispherical cavity were further textured with a knife and re-packed with concrete clumps. Additionally, aggregates up to 0.5 cm in diameter in the concrete mixture contributed to a randomly bumpy overall surface texture. Since Grow Oyster Reef LLC designs products primarily for oyster recruitment, the textural design choices made for these artificial habitat structures were informed by oyster life cycle. Free-swimming larvae spend 14-21 days growing until they attach to surfaces as approximately 0.3 cm

sized spat. Once attached, oysters spend 1-3 years growing into 7 to 13 cm long adults. The size of the hemispherical cavities, as well as the additional surface texture, provide appropriately-sized attachment sites for spat as well as increased surface area for growing oysters.



Figure 3.1: The artificial habitat structures are discs with a 6.4 cm height, a 10 cm diameter, and a 3.2 cm diameter center hole. The center hole facilitates deployment by allowing discs to be strung onto ropes, chains, or pipes.



Figure 3.2: The lateral surfaces of the discs are textured to facilitate recruitment of biodiverse growth. The lateral surface of the discs is textured with two rows of evenly spaced hemispherical cavities that are 2.0 cm in diameter, 0.6 cm in depth from the lateral surface, and 0.5 cm apart. The inner surfaces of each hemispherical cavity were further textured with a knife and re-packed with concrete clumps. Additionally, aggregates up to 0.5 cm in diameter in the concrete mixture contributed to a randomly bumpy overall surface texture.

The Grow Oyster Reef LLC discs were formulated with a patent-pending mix of sand, shale, Portland cement, and ground oyster shells (calcium carbonate). Oyster shell components have been demonstrated to provide an olfactory cue for oyster larval settlement (Hanlon et al. 2019). Standard marine concrete discs will be referred to as “control discs”, and oyster shell-enriched discs will be referred to as “GROW discs.” The control discs were formulated with standard marine concrete, which consists of a mix of sand, shale, and Portland cement.

Thirty replicates of both disc types (control discs and GROW discs) were made. Twenty replicates of each disc type (N=40) were randomly selected to be deployed at Fallon Pier. The other ten replicates of each disc type (N=20) were used for flume experimentation and material strength testing.

### 3.1.2 Field site and permitting

John T. Fallon State Pier, Boston, USA (42.3165° N, 71.0330° W) was selected as the field site for the deployment of artificial habitat structures. The pier is located on the tip of the Columbia Point peninsula in Dorchester Bay, an inlet of Massachusetts Bay. The pier is sheltered from Massachusetts Bay wave energy by the Boston Harbor Islands, a collection of islands situated in Boston Harbor along the same latitude as the pier. Further, Fallon Pier is not affected by any nearby water discharges, such as the elevated water temperatures at Fox Point Pavilion and Boat Dock due to the water discharge from UMass Boston's heating system.

A Construction and Vehicle Access Permit was filed with the Massachusetts Department of Conservation and Recreation to confirm that our experimental design would not cause aesthetic or structural damage to Fallon Pier.

The pier is constructed with wooden railing posts at 1 m intervals on both sides of the pier, which were used to suspend structures that held the discs. Eight wooden railing posts were selected for suspending eight research structures. Once the eight posts were selected, they were marked on the pier. Bathymetry measurements were taken at each of the eight posts in order to ensure that all discs would remain submerged throughout the tidal cycle. In Boston Harbor and Dorchester Bay, the tides are mixed semi-diurnal tides, meaning in each day, one high tide is higher than the other, and one low tide is lower than the other. The mean tidal range at this location is approximately 3.0 m (NOAA Tides and Predictions). Bathymetry measurements were taken at lower low tides. Bathymetry was measured by attaching a 1.4 kg weight to the bottom of a string of twine. The weight was lowered slowly into the water at each marked post, until the bottom was felt. Once the twine was lifted out of the water, measurements were taken of the twine's wetted length. A new dry piece of twine was used for each measurement.

### 3.1.3 Field treatment design

Forty discs were deployed at Fallon Pier, 20 control discs, and 20 GROW. All 40 discs were deployed on August 12, 2019. In order to study seasonal influences on biological recruitment and concrete durability, a subset of discs remained in the field for 3, 6, 11, or 14 months (or 90, 180, 330, or 420 days). The original treatment design called for disc removal after 3, 6, 9, or 12 months with consistent 3-month time intervals, but the COVID-19 pandemic delayed the retrieval of the third and fourth sets of discs. The first set of 10 discs (5 control discs, 5 GROW discs) were removed from the site after 3 months in deployment. The second set of 10 discs were removed from the site 6 months after deployment. The third set of 10 discs were removed from the site 11 months after deployment. The last set of 10 discs were removed from the site after 14 months of deployment. The exact deployment and retrieval dates are listed in Table 3.1.

Table 3.1: 40 discs were deployed at Fallon Pier the on August 12<sup>th</sup>, 2019, 20 of which were control formula discs, and 20 of which were GROW formula discs. A subset of discs remained in the field for 90, 180, 330, or 420 days. The original treatment design called for disc removal after 3, 6, 9, or 12 months with consistent 90-day time intervals, but the COVID-19 pandemic delayed the retrieval of the third and fourth sets of discs.

Retrieval	Deployment date	Retrieval date	Total days deployed
Retrieval 1	8-12-2019	11-10-2019	90
Retrieval 2	8-12-2019	2-9-2020	180
Retrieval 3	8-12-2019	7-8-2020	330
Retrieval 4	8-12-2019	10-6-2020	420

The Fallon Pier experimental design produced a total of eight field treatments for 40 discs: 90-day submersion and GROW formula (90G); 90-day submersion and control formula (90C); 180-day submersion and GROW formula (180G); 180-day submersion and control formula (180C); 330-day submersion and GROW formula (330G); 330-day submersion and control formula (330C); 420-day submersion and GROW formula (420G); 420-day submersion and control formula (420C).

The 40 total discs were hung from the pier with 8 chains, with 5 discs per chain. Each of the 8 hanging chains (referred to as research structures) represented a treatment group. The table below describes which discs were hung on each research structure, and to which treatment group each research structure belonged.

Table 3.2: The Fallon Pier experiment included eight field treatments for 40 discs. The 40 discs were hung from the pier with 8 chains, with 5 discs per chain. Each chain was referred to as a research structure. This table describes which discs were hung on each research structure, and which treatment group each research structure belonged to.

<b>Research Structure</b>	<b>Discs Hung on Research Structure</b>	<b>Treatment Group</b>	<b>Treatment Group Abbreviation</b>
Research Structure #1	Grow #1-5	90-day submersion GROW formula	90G
Research Structure #2	Control #1-5	90-day submersion Control formula	90C
Research Structure #3	Grow #6-10	180-day submersion GROW formula	180G
Research Structure #4	Control #6-10	180-day submersion Control formula	180C
Research Structure #5	Grow #11-15	330-day submersion GROW formula	330G
Research Structure #6	Control #11-15	330-day submersion Control formula	330C
Research Structure #7	Grow #16-20	420-day submersion GROW formula	420G
Research Structure #8	Control #16-20	420-day submersion Control formula	420C

A total of eight research structures were hung from the pier. Each research structure was hung from one of the wooden railing posts with a loop of galvanized steel chain wrapped in protective firehose sleeve tubing (polyurethane sleeve with a polyester cover) to prevent wear on the wood. Each suspension is hung on every other railing post to provide 1 m or 2 m space between suspensions to prevent swaying and knocking of artificial habitat structures into each other.

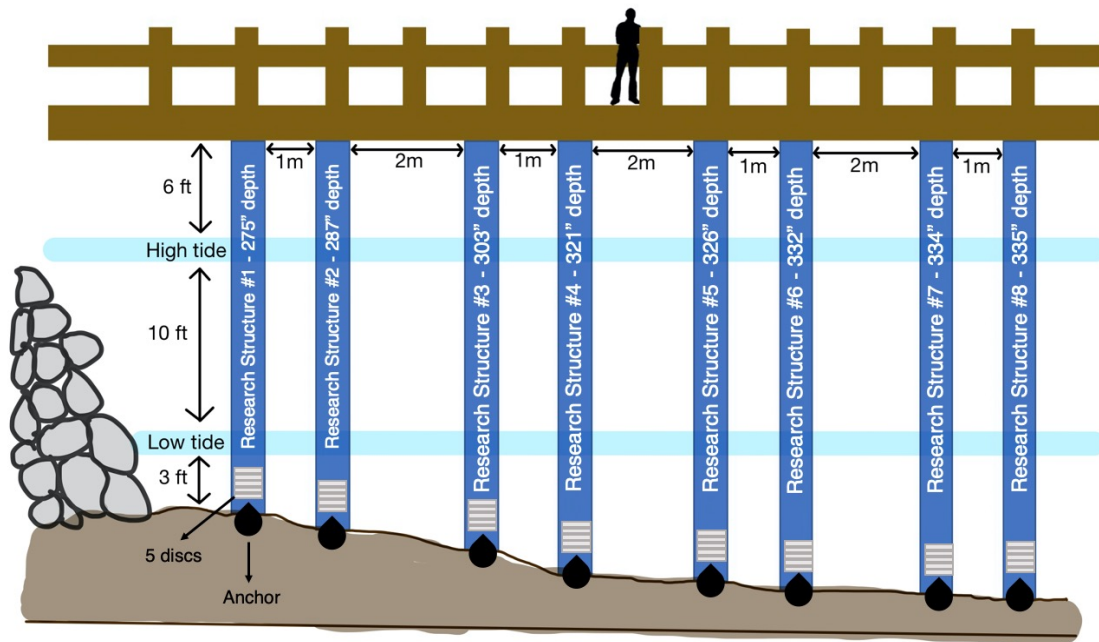


Figure 3.3: A diagram of the experimental setup at Fallon Pier. The vertical blue rectangles represent all eight research structures and their total lengths from the bottom of Fallon Pier to the bed. Research structures were hung with galvanized steel chain. The gray rectangles represent the discs. The light blue horizontal lines mark where mean high tide and mean low tide levels are relative to the pier and to the research structures. The discs were deployed such that they would always be submerged. A 6-foot human figure is included for comparison.



Figure 3.4: South-facing side of Fallon Pier with Research Structure #3 and #4 hung from wooden railing posts with 1 m distance in between.

### 3.1.4 Disc material testing

The discs were subject to material testing prior to and after deployment. A rebound hammer (Humboldt Manufacturing H-2975L Schmidt Hammer, Type L) was used to measure the compressive strength of both control discs and GROW discs. The rebound hammer is a handheld device that measures the compressive strength of concrete, and it is an industry standard for testing marine concrete in-situ. The test is sensitive to local variation in a sample and thus is not considered robust enough to replace the cylinder



compressive strength test. However, it is a valuable test for samples in the field and for samples of unique geometries, such as the reef disc.

The Humboldt Manufacturing H-2975L Schmidt Hammer, Type L is a rebound hammer designed for testing thin-walled structural components with a thickness of less than 10 cm. Since the discs have a height of 7.6 cm, this rebound hammer is suitable for assessing their compressive strength. The discs were placed on a flat surface, and the rebound hammer was compressed four times each at four equidistant points on the top surface (a total of sixteen measurements per disc). Gentle manual force on the end of the rebound hammer activates the internal spring, which impacts the concrete and displays a rebound number. The figure below illustrates how and where the rebound hammer is compressed on each disc.

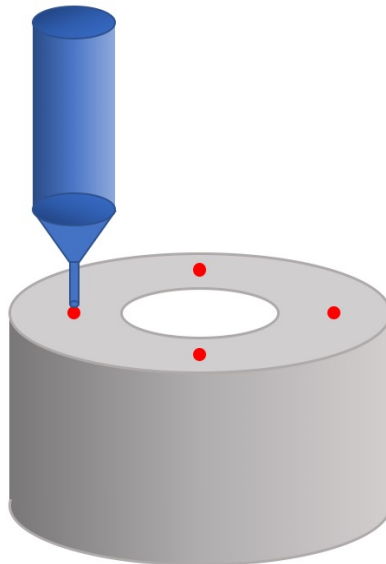


Figure 3.5: The rebound hammer (blue) is applied four times at four equidistant points (red dots) on the top surface (not the lateral surface) of each disc. Gentle manual force on the end of the rebound hammer activates the internal spring, which impacts the concrete and displays a rebound number.

Rebound hammer testing was performed on dry discs before their deployment. After retrieval from Fallon Pier, discs were dehydrated in a 200° C oven, the top and bottom

surfaces were cleaned of biological matter, and discs were tested with the rebound hammer again using the same method.

The rebound hammer displays a rebound number after impact. In order to establish a relationship between rebound number and concrete strength, test cores (cylinder cores of the same concrete material tested) were placed under compression. The rebound hammer was impacted on the cores as they are loaded in compression within a range of loads from zero to half of the load at material failure. Plotting rebound number (x) versus compressive load (y) produced a correlation curve that was used for translating rebound numbers to values of compressive strength in Megapascals. The GROW and control materials produced the same correlation curves. Figure 3.6 shows the correlation curve plot generated from test core compressions.

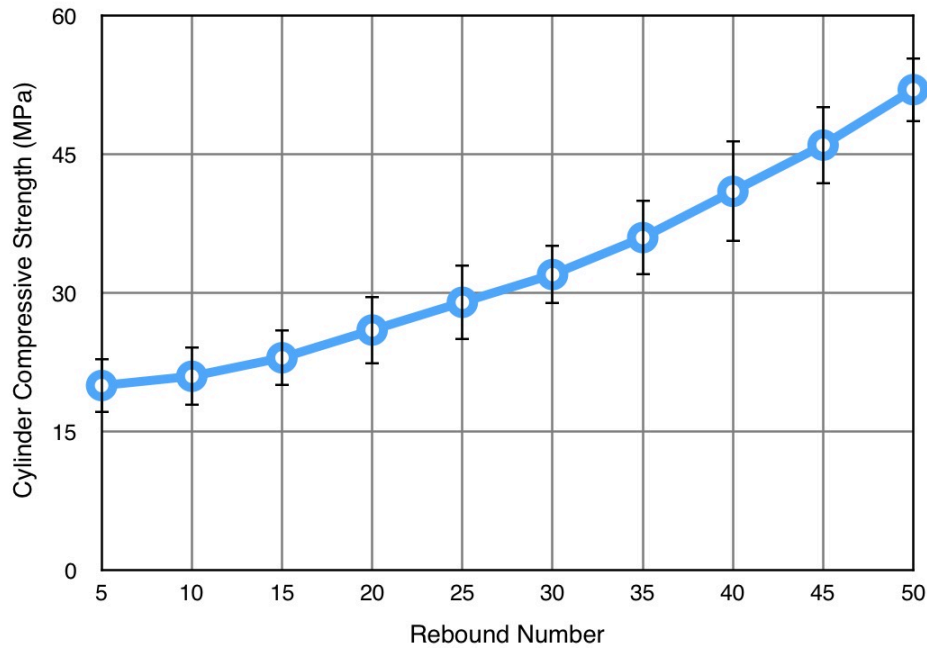


Figure 3.6: Correlation curve for the Humboldt Manufacturing H-2975L Schmidt Hammer, Type L on GROW and control material test cylinders. Rebound numbers are correlated to compressive strength in units of MPa. The GROW and control materials produced the same correlation curves.

Cylinder compressive strength testing was also performed, using test cylinders cast from the same control and GROW formulas as the discs. The test cylinders were first capped

with plaster of Paris to ensure smooth and perpendicular top and bottom surfaces for flush contact with the surfaces of the Instron machine. This is important because slight imperfections such as a slanted surface or texture can reduce the surface area that load is being applied on and cause material failure to occur prematurely. After the plaster of Paris caps dried, the test cylinders were loaded onto the Instron machine and subjected to compressive loads increasing from 0 N to load at material failure at a rate of 0.2 MPa/sec. Four test cylinders of each material type, control and GROW, were compressed. The load at failure was recorded for each test cylinder. The failure loads will be compared to rebound hammer measurements in the analysis.

The same plaster surface preparation procedure and compressive strength testing was performed on three untreated discs of each material, using the Instron machine. GROW and control discs retrieved from the field were also subjected to Instron compressive strength testing for comparison to rebound hammer testing results.

### **3.1.5. Disc identification**

Each disc was assigned an identification code. The 20 control discs were C1 through C20. The 20 enriched concrete GROW discs were G1 to G20. The mass and rebound number of each disc was recorded along with its identification code.

A sheet of 0.3 cm (1/8") thick commercial grade Rubber-Cal Neoprene was stamped with 5 cm and 2.5 cm diameter leather punches to create rubber washers, which were used as part of the hanging research structures. The identification codes were branded onto rubber washers with a soldering iron so that the identification of each disc could be confirmed after deployment and retrieval.



Figure 3.7: Rubber washers were made of 0.3 cm (1/8") thick commercial grade Rubber-Cal Neoprene and were stamped with 5 cm and 2.5 cm diameter leather punches. The labeling of disc identification codes is visible on the top row of rubber washers.

### 3.1.6. Construction of hanging research structures

Each disc was fitted with 1" nominal PVC pipe through the center hole to prevent damage to the disc via abrasion from the chain. The inner diameter of the discs ranged from 3.4 cm to 3.8cm, and the outer diameter of 1" nominal PVC piping is 3.3 cm, thus the PVC piping fit securely inside the discs. PVC pipe was cut to the height of the discs, then inserted into the center hole via gentle tapping with a rubber mallet. The inner surface of the center holes had slight textural imperfections, thus requiring insertion via rubber mallet tapping for the majority of the discs.



Figure 3.8: Each disc was fitted with 1” nominal PVC pipe through the center hole to prevent damage to the disc via abrasion from the chain.

Grade 30 galvanized steel coil chain was selected for hanging discs because of its corrosion-resistant coating, and because the 0.6 cm (1/4”) chain fit snugly inside the PVC pipe. The chain was cut to length based on the eight bathymetry measurements taken at each piling. A length of 0.5 m of chain at the end was used for attaching the discs. Discs were strung onto the chain and fixed in place along the chain with a piece of threaded rod bolted into the exposed chain link above and below the disc. In order to protect the disc from abrasion from the threaded rod and bolts above and below each disc, labeled rubber washers were placed against the top and bottom of every disc. The chain was cut to eight segments of 4 feet, for the loop around the pilings. These 1.2-m segments of chain were covered by firehose sleeves to prevent damage to the wooden pier railings. A 15-kg anchor was attached to the bottom end of each chain with shackles. The anchor weight was selected shackles were tightened then seized with seizing wire.



Figure 3.9: Five discs were strung onto each chain segment and fixed in place along the chain with a piece of threaded rod bolted into the exposed chain link above and below the disc.

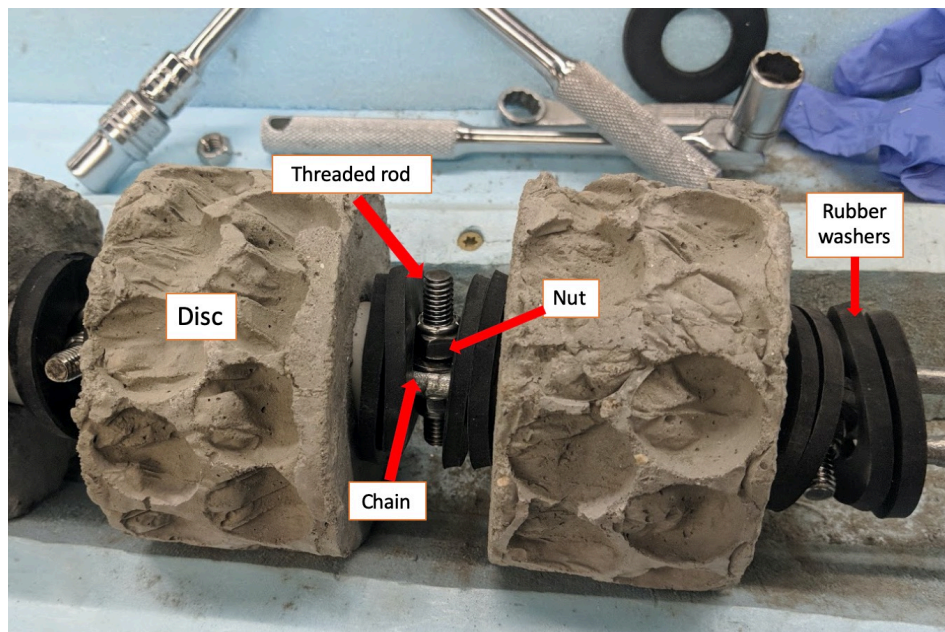


Figure 3.10: Rubber washers provide protection against abrasion from the threaded rod and nuts. The threaded rod and nuts secure each disc's location on the chain.



### 3.1.7. Deployment and retrieval of hanging research structures on John T. Fallon State Pier

The chain loop covered with fire hose sleeve was looped around the wood piling and closed off with a shackle, which was then tightened and seized. Each research structure was lowered off the pier by a small forklift that was balanced with a 60-kg counterweight. When the research structure was around halfway down, the top of the chain was connected by a shackle to the shackle closing the chain loop around the piling. The shackle was tightened and seized. The rest of the research structure was lowered into the water.



Figure 3.11: The small forklift used to lower and lift hanging research structures from the pier into the water. A 60-kg counterweight was used to balance the forklift.

Upon retrieval, each disc was placed individually in a watertight container filled with seawater collected at Fallon Pier. The containers were pre-labeled with the

corresponding code for each disc (C1 to 20, and G1 to 20). Any mobile organisms, such as crabs or fish that fell off the discs onto the floor of the pier, were placed immediately in containers of seater. Discs were transported in their individual seawater-filled containers and were immediately refrigerated at MIT Seagrant. Each disc was taken out of the refrigerator individually to be photographed for no more than ten minutes at a time to reduce death of organisms due to temperature change.

The photographing procedure involved taking a photo of the top surface, bottom surface, and four photos of the lateral surface. The lateral surface of the disc was separated into four quadrants, and each was photographed once. All photographs were taken on an iPhone 11 in direct sunlight through a window while discs were submerged in clean water. After photos were complete, the disc was returned to its individual container of seawater and refrigerated. After two days in the refrigerator, discs were preserved in ethanol.

### **3.1.8. Sampling**

After retrieval and transfer to MIT SeaGrant, discs were individually analyzed under a 10x to 40x microscope. The percent coverage of each species present at the surface was measured systematically using a grid of 100 equidistant points. The lateral surface of each disc was divided into four equal quadrants and marked with rubber bands.

Twenty-five equidistant grid spots were printed on a clear acetate sheet that was placed on top of each quadrant, and held in place by the rubber bands while each disc was studied under the microscope. The species located directly under each grid spot was recorded. For areas with overlapping species, only the species on the top layer was recorded. Once the species were recorded at each of the 25 grid spots for a quadrant, the disc was rotated and the acetate sheet was placed on the next quadrant. This was repeated for four quadrants on each disc until analysis of a total of 100 grid points was completed. The 100 point measurements on each disc were used to calculate the percent coverage of each species on that disc. For example, if species A had a count of 20 points



on disc #1, disc #1 had a percent coverage of 20% for species A (Elzinga et al. 1998). In addition to percent coverage, a presence/absence list of all observed species was recorded for each disc.

After percent cover analysis was conducted, discs were dehydrated in a 200° C dehydration oven. Dehydration causes most of the softer tissues to fall off, leaving behind calcareous growth. Once only calcareous growth remained on discs surfaces, the percent cover analysis was conducted again to count percent cover of calcareous growth.

### **3.1.9. Flume experiments to measure CaCO<sub>3</sub> leaching from discs**

Experiments were conducted in a flume with the purpose of measuring the CaCO<sub>3</sub> leaching potential of GROW and control discs.

A calcium ion-selective electrode was calibrated with a high Ca ISE solution of 1000 mg/L and then when a low Ca ISE solution of 10 mg/L. Measurements from the calcium ion-selective electrode were read from a Thermo Fisher 0710A0 Benchtop Meter. The calcium ion-selective electrode took measurements in millivolt units, which were converted to units of ppm Ca<sup>2+</sup> in Matlab R2016b using a log-linear fit of the calcium ion-selective electrode calibration curve.

Three 18 cm x 18 cm x 15 cm aquariums were used to measure calcium leaching of discs in still water. One aquarium contained a single control disc in 1 L of deionized water, one contained a single GROW disc in 1 L of deionized water, and one contained 1 L of deionized water only. The deionized water was confirmed to have a conductivity of 0.0 microSiemens/cm with a conductivity probe before it was poured into the three aquariums. After 72 hours, the discs were removed from the aquariums, then the water was stirred manually and tested with the calcium ion-selective electrode. The three aquariums were then flushed, refilled with new deionized water, and subjected to the

same three treatments. After 24 hours, the water in each aquarium was tested with the calcium ion-selective electrode and with the conductivity probe again.

A flume was used to measure calcium leaching of discs in moving water. The flume has a 3-m long test section with 38-cm width and can accommodate flow depths up to 40 cm. A flume test with 5 discs, control or GROW, sitting on the bed of the flume was performed to determine the rate of calcium carbonate dissolution of control and GROW discs in mild currents. 5 discs of the same material type were set on the bed of the flume, at the center of the test section. The water height was set to 7 cm, which provided 1cm of water flow above the height of the discs.

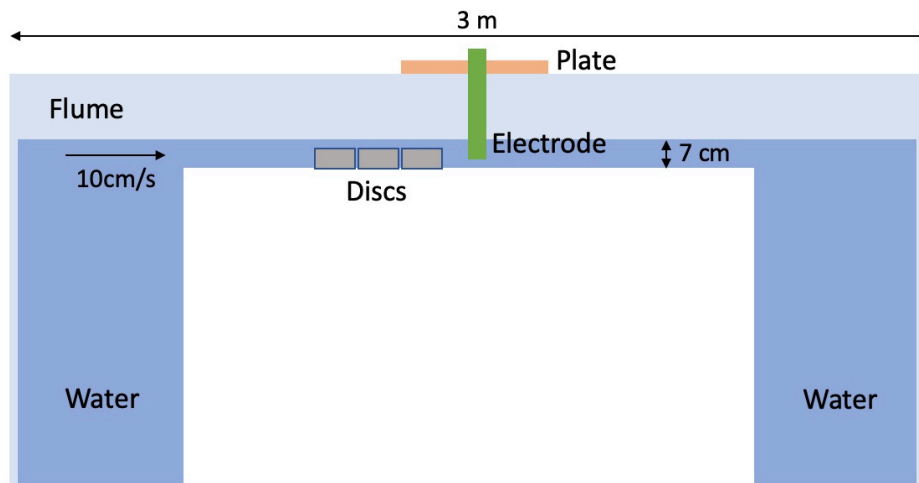


Figure 3.12: Side-view of the flume. The test section is 3 m long. The plate securely holds the calcium-ion selective electrode with the electrode tip 5 cm downstream from the discs and 3.5 cm from the water surface. The water velocity was 10 cm/s. The water depth was 7 cm, which provided 1cm of water flow above the height of the discs. From the side-view there appears to be three discs, but there are five discs on the bed of the flume.

The calcium-ion selective electrode was plugged into the benchtop meter and then secured to a plate above the flume, with the electrode tip 5 cm in front of the discs in the direction of water flow, and at a depth of 3.5 cm from the water surface. The water velocity was 10 cm/s. For comparison, Dorchester Bay typically experiences tidal currents ranging from 20 cm/s to 40cm/s in velocity at a depth of 3 m (NOAA Tides and Currents, City Point Buoy). For an open channel with rectangular cross section, such as the flume, the Reynolds number is defined by:

$$Re = \frac{vd_h}{\nu}$$

$$d_h = \frac{4A}{P}$$

in which  $v$  is the water velocity,  $\nu$  is the kinematic viscosity of water,  $d_h$  is the hydraulic diameter,  $A$  is the cross-sectional area and  $P$  is the wetted parameter of the channel. A Reynolds number greater than 4000 indicates turbulent flow. For the test conditions used in this study, (38-cm width, 7-cm depth, and 10-cm/s)  $Re = 19426$ , indicating fully turbulent flow.

A fixed volume of water was re-circulated in a closed system so that the loss of ions from the reef discs could be inferred from the increasing concentration in the water. The flume was run at 10 cm/s until the calcium ion-selective electrode measurements reached a plateau. The calcium ion-selective electrode took measurements every 30 seconds for the first 2 minutes, then every 1 minute for 60 minutes, and then every 10 minutes until measurements plateaued. Once measurements plateaued, the flume was drained, refilled to a water height of 7 cm, and the same procedure was repeated with the same 5 discs. The procedure was repeated for a total of three runs.

The increase in calcium and carbonate ion concentrations was calculated by subtracting background concentrations in tap water from final concentrations.

## 3.2 Statistical Analysis

The experimental design produced eight field treatments for 40 discs: 90-day submersion and GROW formula (90G); 90-day submersion and control formula (90C); 180-day submersion and GROW formula (180G); 180-day submersion and control formula (180C); 330-day submersion and GROW formula (330G); 330-day submersion and control formula (330C); 420-day submersion and GROW formula (420G); 420-day submersion and control formula (420C).

Five discs were in each treatment group. Point count data were converted from counts (100 points sampled/disc, 500 points sampled/treatment) into percent cover for each species present. The software package PRIMER-E v.7 was used to construct a Bray-Curtis similarity matrix with a square root transformation of percent cover data. A non-metric multidimensional scaling (nMDS) ordination was used to visualize relationships among treatment groups. SIMPER analysis was performed to examine the contribution of individual species or functional groups to the dissimilarity of community composition among treatment groups.

### 3.2.1 Bray-Curtis similarity matrix

The Bray-Curtis coefficient is a similarity measure commonly used in ecology. Originally introduced by Bray and Curtis in 1957, the coefficient is defined as:

$$BC_{ij} = 100 \frac{2Z_{ij}}{S_i + S_j}$$

in which  $S_i$  and  $S_j$  are the total number of species or functional groups at site or treatment  $i$  and  $j$ , respectively, and  $Z_{ij}$  is the sum of the lowest species or functional group count for each site.  $BC_{ij}$  is a percentage, where 0% means the two sites or treatments do not share any species, and 100% means they have the same species composition.

The Bray-Curtis coefficient can be calculated from raw percentage cover data, but in unbalanced communities where there are a small number of very abundant species, the contribution of less abundant species to similarity can be lost. Pre-treatment of percentage cover data via a square root transform (also called double root transform) or 4<sup>th</sup> root transform has the effect of damping the importance of the highly abundant species, so that similarities depend on rarer species as well.

### **3.2.2. Non-metric Multidimensional Scaling (nMDS)**

nMDS is an ordination method which orders multivariate objects (ie. treatment groups) so that similar objects are close to each other and dissimilar objects are far from each other, calculated based on a similarity or dissimilarity matrix such as a Bray-Curtis matrix. On an nMDS plot, objects that are ordinated closer to one another are likely to be more similar than those further apart. However, the scale of the axes is arbitrary as is the orientation of the plot.

### **3.2.3 SIMPER analysis**

The similarity percentages breakdown (SIMPER) procedure (Clarke 1993) assesses the average percent contribution of individual species or functional groups to the dissimilarity between multivariate objects (ie. treatment groups) in a Bray-Curtis dissimilarity matrix. SIMPER reveals which species are likely to be the major contributors to differences community composition between treatment groups.

### **3.2.4. Independent t-tests**

T-tests were performed on material strength testing data to determine if the GROW and control materials had statistically significant differences in compressive strength. A t-test is a statistical test used to compare two groups of means to determine if a treatment (in our case, the addition of CaCO<sub>3</sub>) has an effect on the parameter of

interest (compressive strength). Since the two groups of means tested are independent of each other, we used a two-sample t-test, also known as an independent t-test. The t-test calculates a p-value, which is the probability that the results from the data occurred by chance. For the selected confidence interval of 95%, a p-value of 0.05 (5%) or lower indicates the two means being compared are different, while a p-value higher than 0.05 indicates the two means have no statistically significant difference.

# Chapter 4

## Results

### 4.1 Observations from Field Deployment

Research structures were photographed immediately upon removal from the pier. Figure 4.1 presents photographs of GROW research structure from each of the four retrievals.



Figure 4.1: GROW research discs retrieved from Fallon Pier. Left-to-right: 90-day, 180-day, 330-day, 420-day retrievals on November 14<sup>th</sup>, 2019, February 12<sup>th</sup>, 2019, July 8<sup>th</sup>, 2020, and October 6<sup>th</sup>, 2020 respectively.

A total of 16 functional groups were observed over the eight treatment groups. Presence/absence data for each treatment group lists every observed organism (Table 4.1). Photographs of the functional groups are included (Table 4.2).

Table 4.1: List of organisms observed on the five discs of each treatment group. Bolded headers indicate which treatment group the column represents.

<b>90C</b> (control, 3 months)	<b>90G</b> (GROW, 3 months)	<b>180C</b> (control, 6 months)	<b>180G</b> (GROW, 6 months)
<i>Didemnum sp.</i>	<i>Didemnum sp.</i>	<i>Didemnum sp.</i>	<i>Didemnum sp.</i>
<i>Botrylloides violaceous</i>	<i>Botrylloides violaceous</i>	<i>Botrylloides violaceous</i>	<i>Botrylloides violaceous</i>
<i>Asciidiella aspersa</i>	<i>Asciidiella aspersa</i>	<i>Asciidiella aspersa</i>	<i>Asciidiella aspersa</i>
Tubes	Tubes	Tubes	Tubes
Barnacles	Barnacles	Barnacles	Barnacles
Red filamentous algae	Red filamentous algae	Red filamentous algae	Red filamentous algae
Brown filamentous algae	Brown filamentous algae	Brown filamentous algae	Brown filamentous algae
Green leafy algae	Green leafy algae	Green leafy algae	Green leafy algae
Hydroid		Hydroid	Hydroid
<i>Styela clava</i>		<i>Styela clava</i>	Kelp
European green crab		Kelp	
Fish (unidentified)			
<b>330C</b> (control, 9 months)	<b>330G</b> (GROW, 9 months)	<b>420C</b> (control, 12 months)	<b>420G</b> (GROW, 12 months)
<i>Didemnum sp.</i>	<i>Didemnum sp.</i>	<i>Didemnum sp.</i>	<i>Didemnum sp.</i>
<i>Botrylloides violaceous</i>	<i>Botrylloides violaceous</i>	<i>Botrylloides violaceous</i>	<i>Botrylloides violaceous</i>
<i>Styela clava</i>	<i>Styela clava</i>	<i>Styela clava</i>	<i>Styela clava</i>
<i>Asciidiella aspersa</i>	<i>Asciidiella aspersa</i>	<i>Asciidiella aspersa</i>	<i>Asciidiella aspersa</i>
Tubes	Tubes	Tubes	Tubes
Barnacles	Barnacles	Barnacles	Barnacles
Kelp	Kelp	Kelp	Kelp
Mussels	Mussels	Mussels	Mussels
European green crab	European green crab	Red leafy algae	Common slipper shell
Common slipper shell	Common slipper shell	Common slipper shell	



Table 4.2: Photographs of observed organisms on retrieved discs. Photos captured with an iPhone 11 camera without magnification (*Didemnum* sp., *Asciidiella aspersa*, *Botrylloides violaceous*, kelp, mussels, *Styela clava*, European green crab, common slipper shell) or with 10x magnification (Hydroid, barnacle, tubes, algae).

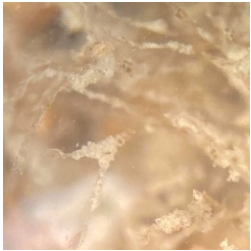



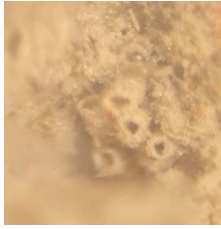







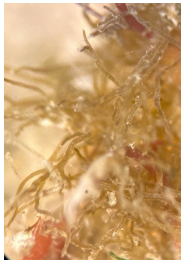


Hydroid	Barnacle	<i>Didemnum</i> sp.	<i>Asciidiella aspersa</i>	Tubes
				
Green leafy algae	Kelp	Mussels	<i>Styela clava</i>	European green crab
				
Common slipper shell	Red leafy algae	Brown filamentous algae	<i>Botrylloides violaceous</i>	Red filamentous algae
				

Table 4.3: Abbreviations for functional group and species names. The species and functional group names were abbreviated for plotting purposes, and the abbreviations are listed below in the second column. The common name is included in the third column for reference.

Functional group name	Abbreviation for plots	Common name
<i>Didemnum</i> sp. *	di	Carpet sea squirt
Tubes <sup>†</sup>	tubes	-
<i>Styela clava</i>	sty	Club tunicate
<i>Ascidrella aspersa</i>	asc	European sea squirt
<i>Botrylloides violaceus</i>	bv	Red-orange sheath tunicate
Barnacles	ba	-
Kelp	kelp	-
Hydroid	hy	-
Green leafy algae	GLA	-
Red filamentous algae	RFA	-
Brown filamentous algae	fbrown	-
Red leafy algae	RLA	-
Bare substrata	bare	-

\* *Didemnum* sp. is likely *Didemnum vexillum*, which has been observed to have great presence in New England waters since the 1980s (Kennedy et al. 2020).

<sup>†</sup>Note that “tubes” refer to the organic tube structures constructed by crustaceans of the Corophiidae family. Several crustacean species build delicate tubes to inhabit, using fibrous secretions from their limbs ( Bastidas, interview/discussion 2020, “Tanaid” 2009).

## 4.2 Percent Cover

### 4.2.1 Top Surface Layer

The surfaces of discs from all treatment groups were typically dominated by three species, but the species differed between treatments. For each treatment group, the top three species covered at least 65% of the total surface of five discs.

After 90 days in the field, the control and GROW discs were both dominated by hydroids, barnacle and tubes. Specifically, for the control discs, hydroids, barnacles, and tubes occupied 36%, 21.2%, and 17.8% of the surface, respectively. For the GROW

discs, barnacles, hydroids, and tubes occupied 33.8%, 19.4%, and 11.8% of the surface, respectively.

After 180 days in the field, the control and GROW discs were both predominantly covered with tubes and *Didemnum* sp. Specifically, for the control discs, tubes, *Didemnum* sp., and red-orange sheath tunicate occupied 33.6%, 16.2%, and 15.6% of the surface, respectively. For the GROW discs, tubes, *Didemnum* sp., and barnacles occupied 42.8%, 16.4%, and 10.6% coverage respectively.

After 330 days in the field, the control and GROW discs were both predominantly covered with red-orange sheath tunicates and Eastern sea squirts. Specifically, for the control discs, red-orange sheath tunicates, Eastern sea squirts, and tubes occupied 35%, 13.6%, and 12.6% of the surface, respectively. For the GROW discs, Eastern sea squirts, red-orange tunicates, and *Didemnum* sp. occupied 33%, 31.6%, and 20.4% of the surface, respectively.

After 420 days in the field, the control and GROW discs were both predominantly covered with *Didemnum* sp. and tubes. Specifically, for the control discs, *Didemnum* sp., tubes, and Eastern sea squirts occupied 59%, 19.2%, and 12% of the surface, respectively. For the GROW discs, *Didemnum* sp., tubes, and Eastern sea squirts occupied 55.8%, 18%, and 10% of the surface, respectively.

The percent cover bar graph (Figure 4.2) provides quantitative insight into seasonal trends of recruitment. Seasonal trends in species coverage were similar for control and GROW treatments. *Didemnum* sp. coverage increased with increasing submersion time. Hydroids exhibited peak coverage after 90 days of submergence, tubes exhibited peak coverage after 180 days of submergence, and ascidians exhibited peak coverage during the 330 days of submergence.

Table 4.4: Average percent cover of the surface, organized by treatment group. Each treatment group had five deployed discs. The surface of each disc was sampled at 100 points. The average percent cover was calculated by summing data over 500 total points and dividing by 5 discs to produce percent cover equaling 100 in this table. Species names have been abbreviated according to Table 4.3. The first number reported is the average percent cover, and the number in brackets is the standard deviation.

	<b>90G</b>	<b>180G</b>	<b>330G</b>	<b>420G</b>	<b>90C</b>	<b>180C</b>	<b>330C</b>	<b>420C</b>
<b>di</b>	11.8 (6.3)	16.4 (3.3)	20.4 (6.2)	55.8 (16)	16.6 (4.0)	16.2 (5.8)	29 (13)	59 (15)
<b>tubes</b>	22.0 (6.5)	42.8 (7.5)	4.8 (2.2)	18 (11)	17.8 (6.3)	33.6 (7.6)	12.6 (3.8)	19.2 (4.5)
<b>sty</b>	0	1.2 (1.2)	2.8 (2.8)	8.6 (6.1)	0.2 (0.4)	1.2 (1.3)	4.8 (5.9)	3.2 (3.2)
<b>asc</b>	2.2 (2.1)	9.8 (4.3)	33 (13)	10 (10)	3.0 (2.2)	15.0 (9.0)	13.6 (6.0)	12 (14)
<b>bv</b>	1.8 (1.6)	9.8 (4.5)	31.6 (5.9)	3.6 (3.5)	0.6 (0.8)	15.6 (2.8)	35 (14)	3.4 (4.1)
<b>ba</b>	33.8 (3.3)	10.6 (6.4)	1.0 (1.2)	4 (3.7)	21.2 (2.6)	3.6 (2.4)	3.4 (2.5)	3.4 (2.9)
<b>kelp</b>	0	0	6 (12)	0	0	0	1.4 (1.7)	0
<b>hy</b>	19.4 (7.5)	3.2 (3.5)	0	0	36 (10)	11 (13)	0	0
<b>GLA</b>	4 (2.0)	5.4 (3.8)	0	0	0.2 (0.4)	0	0	0
<b>RFA</b>	0.6 (0.8)	0	0	0	2 (3.5)	0	0	0
<b>fbrown</b>	0.4 (0.8)	0	0	0	0.2 (0.4)	0	0	0
<b>RLA</b>	0	0	0	0	0.4 (0.5)	0	0	0
<b>bare</b>	4.2 (1.7)	0.8 (1.2)	0	0	1.4 (0.8)	1 (0.7)	0	0

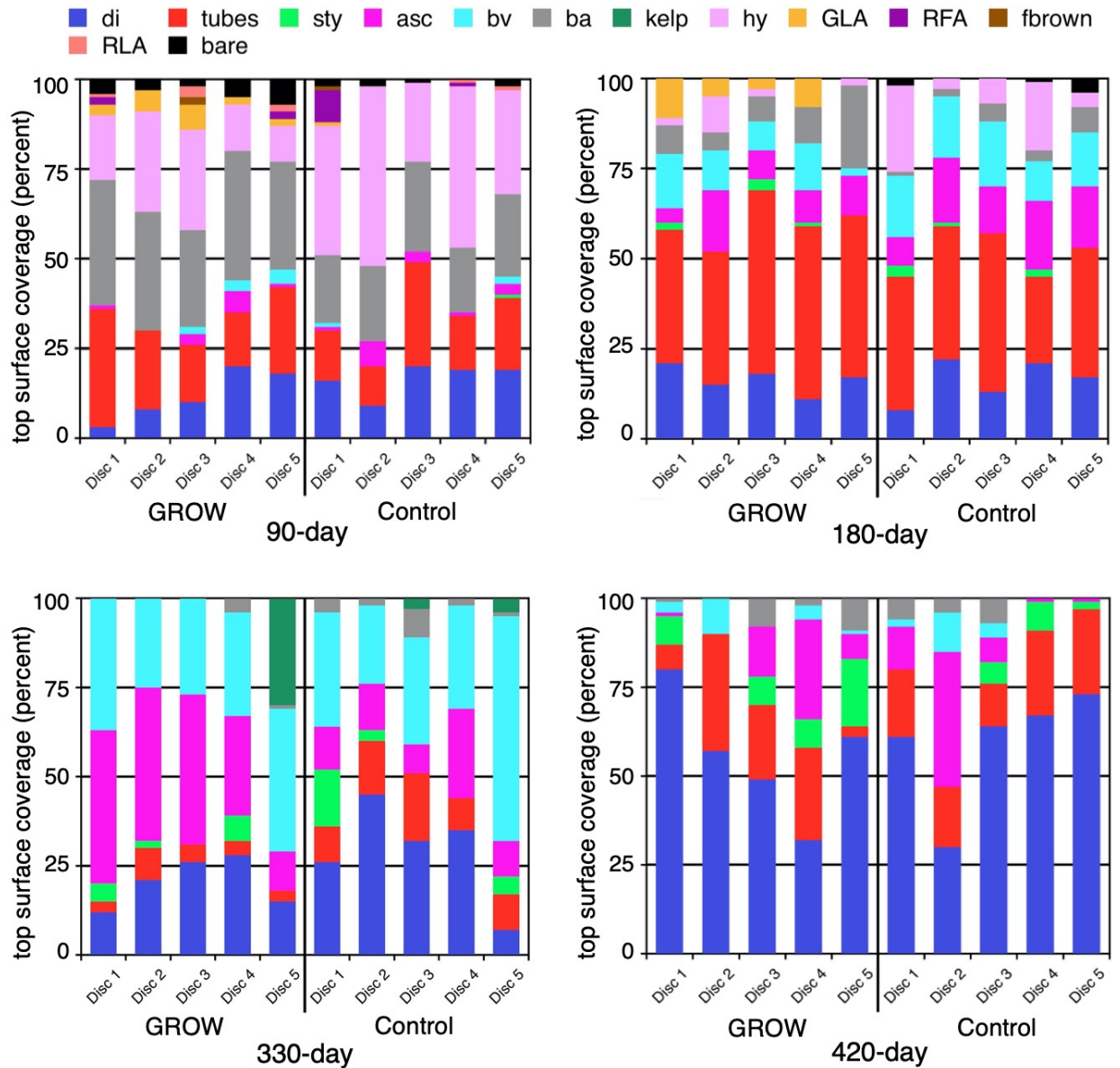


Figure 4.2. Percent cover of benthic functional groups for every disc deployed.

### 4.2.2 Innermost Surface Layer

After the top surface of all discs were studied for percent coverage, discs were dehydrated to reveal only calcareous recruitment. Percent coverage of calcareous recruitment on the concrete surface (innermost layer of recruitment) was recorded.



Figure 4.3: A disc from treatment group 420G that has been dehydrated to reveal only calcareous recruitment. The top surface of this disc from treatment group 420G is almost entirely colonized by barnacles.



Figure 4.4: On the left is a dehydrated disc from treatment group 420G, on the right is a dehydrated disc from treatment group 180G. Barnacle percent coverage on the innermost surface increased with submersion time.



Table 4.5: Average percent cover of calcareous recruitment on concrete surface as observed after disc dehydration and removal of all non-calcareous growth. Three out of five discs from each of the eight treatment groups was tested with the rebound hammer because of the labor-intensive surface preparation process. The first number reported is the average percent cover, and the number in brackets is the standard deviation.

90G	180G	330G	420G	90C	180C	330C	420C
33.8 (5.6)	50.9 (4.2)	73.3 (6.7)	81.1 (9.8)	21.2 (4.9)	40.5 (5.7)	66.7 (10.1)	86.4 (8.3)

Table 4.6: Counts and sizes of mussels observed on discs retrieved from the 330-day and 420-day submersion group.

330G				
Disc 1	Disc 2	Disc 3	Disc 4	Disc 5
3 - < 1 cm	0	0	2 - < 1 cm	3 - < 1 cm
420 G				
Disc 1	Disc 2	Disc 3	Disc 4	Disc 5
2 - 4 cm 1 - 3 cm 2 - 2 cm 3 - <1 cm <b>8 total</b>	1 - 2cm 5 - < 1 cm <b>6 total</b>	1 - 4 cm 2 - 3 cm 3 - < 1 cm <b>6 total</b>	1 - 2 cm 6 - < 1 cm <b>7 total</b>	1 - 3 cm 1 - 2 cm 3 - < 1 cm <b>5 total</b>
330C				
Disc 1	Disc 2	Disc 3	Disc 4	Disc 5
0	0	0	3 - <1 cm	3 - < 1 cm
420 C				
Disc 1	Disc 2	Disc 3	Disc 4	Disc 5
1 - 2 cm <b>1 total</b>	0	1 - 4 cm <b>1 total</b>	3 - < 1 cm <b>3 total</b>	1 - 3 cm 1 - 2 cm <b>2 total</b>

### 4.3 Multivariate Analysis

Bray-Curtis similarity calculations and nMDS ordination found that treatment groups 330C and 330G (330-day control and 330-day GROW) had highly similar species composition, as did treatment groups 420C and 420G (420-day control and 420-day GROW), suggesting that submersion time had greater influence on species composition and recruitment than material in these treatment groups. nMDS ordination also found that treatment groups 180C and 180G are more similar to each other than to any other treatment groups, and that 90C and 90G are more similar to each other than to any other treatment groups.

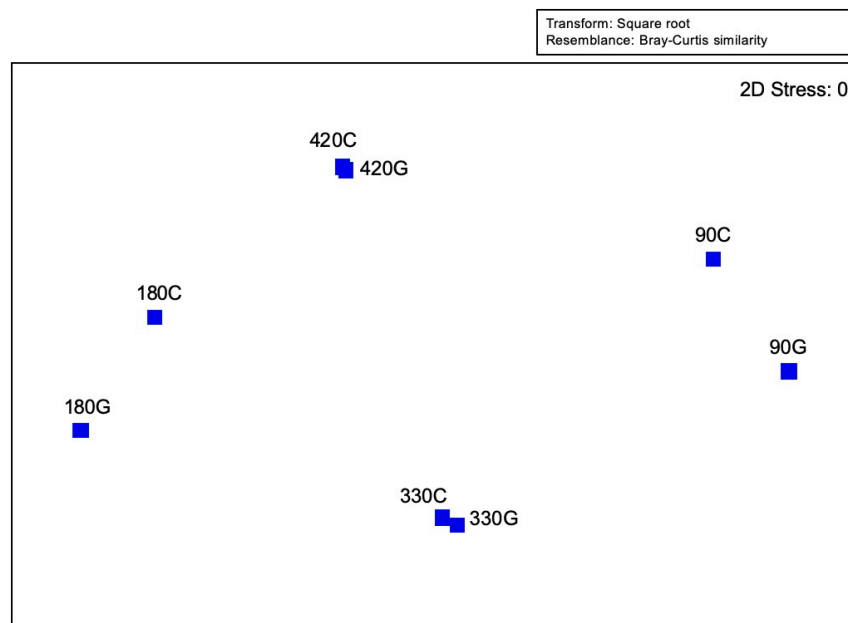


Figure 4.5: nMDS plot for eight multivariate objects (eight treatment groups). Points represent treatment groups. Treatments groups that are more similar to one another are ordinated closer together. The axes and orientation are arbitrary. Treatment groups 330C and 330G are highly similar to each other, as are treatment groups 420C and 420G.

SIMPER analysis revealed that control and GROW treatment groups were highly similar (>80% similarity) across all submersion times, suggesting that material enrichment with calcium carbonate was less influential on species composition than



submersion time. Percent contribution to dissimilarity by the most abundant species (main contributing species) increased as submersion time increased (Table 4.7), indicating that as discs were submerged longer, the disc surface became increasingly dominated by a single species, making the surface homogenous and less diverse, but that the dominant species changed over time.

SIMPER analysis between submersion time-lengths regardless of material revealed that there were significant differences in species composition due to differences in submersion times (Table 4.8).

Table 4.7: SIMPER analysis compared similarity in species composition between treatments with the same submersion time but different material. SIMPER calculates average similarity as a percentage, and also the % contribution to the dissimilarity by species. Take the comparison of 90C and 90G as an example: these two treatment groups had an average similarity in species composition of 81.52%, with barnacles contributing to 21.15% of the dissimilarity between the two treatment groups.

	Average similarity (%)	Main contributing species	Contribution (%)
90C and 90G	82	Barnacles	21
180C and 180G	85	Tubes	27
330C and 330G	85	<i>Botrylloides violaceous</i>	28
420C and 420G	95	<i>Didemnum</i> sp.	37

Table 4.8: SIMPER analysis data for comparing similarity in species composition between treatments with different submersion times regardless of material.

	Average similarity (%)	Main contributing species	Contribution (%)
90-day and 180-day	32	Hydroid	16
90-day and 330-day	56	Hydroid	18
180-day and 330-day	33	Tubes	21
90-day and 420-day	47	Hydroid	23
180-day and 420-day	30	<i>Didemnum</i> sp.	25
330-day and 420-day	28	<i>Botrylloides violaceous</i>	32

#### 4.4 Flume Experimentation

Three 18 cm x 18 cm x 15 cm aquariums were used to measure calcium leaching of discs in still water. One aquarium contained a single control disc in 1 L of deionized water, one contained a single GROW disc in 1 L of deionized water, and one contained 1 L of deionized water only. The calcium ion concentration was measured for 24 hours of submersion and 72 hours of submersion, in order to gauge the ion leaching potential of the disc materials relative to the  $\text{CaCO}_3$  dissolution equilibrium, the tap water background concentrations, and the calibrating solutions (Figure 4.6).

Table 4.9: Calcium ion concentration was measured for 24 hours of submersion and 72 hours of submersion for single discs of control and GROW material in still water 18 cm x 18 cm x 15 cm aquariums.

Time Submerged in Aquarium	Control Disc	GROW Disc
24 hours	334 ppm $\text{Ca}^{2+}$	76 ppm $\text{Ca}^{2+}$
72 hours	505 ppm $\text{Ca}^{2+}$	198 ppm $\text{Ca}^{2+}$

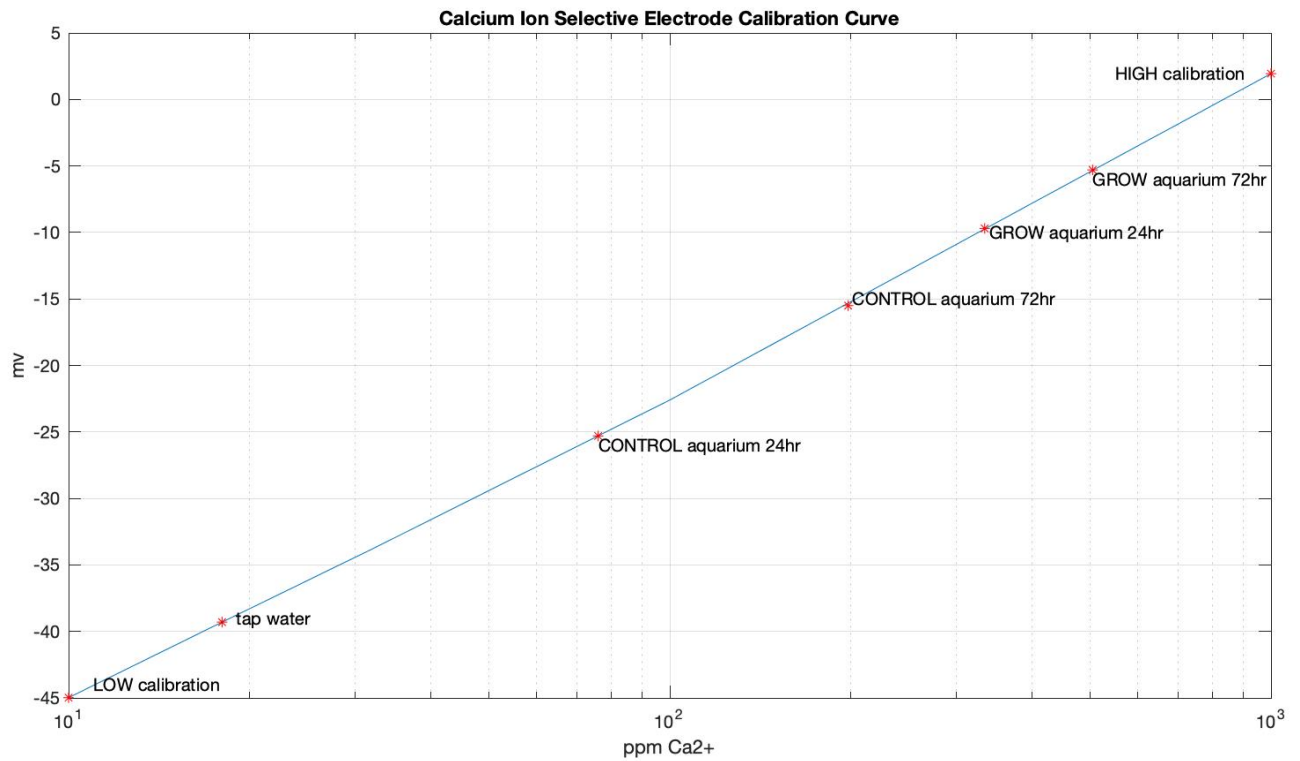


Figure 4.6: Calibration curve of the calcium ion selective electrode. The electrode takes measurements in millivolts, which has a log-linear relationship with concentration in ppm. The low concentration calibration solution (10 ppm), high concentration calibration solution (1000 ppm), tap water, and aquarium concentrations are mapped on the calibration curve for comparison.

A fixed volume of water was re-circulated in a closed system so that the loss of ions from the reef discs could be inferred from the increasing concentration in the water. The flume was run at 10 cm/s until the calcium ion-selective electrode measurements reached a plateau. Figure 4.7 below plots the calcium ion concentration with time for 5 GROW discs that were subjected to three continuous runs in the flume at 10 cm/s water velocity. Figure 4.8 below plots the calcium ion concentration with time for 5 control discs that were subjected to three continuous runs in the flume at 10 cm/s water velocity.

5 GROW discs subjected to turbulent flow conditions were able to increase calcium ion and carbonate ion concentrations by  $8.7 \times 10^{-5}$  M within 100 minutes in the first flush, before plateauing. In the second flush, calcium ion and carbonate ion concentrations increased by  $6.1 \times 10^{-5}$  M within 40 minutes before plateauing. In the third flush, calcium ion and carbonate ion concentrations increased by  $6.1 \times 10^{-5}$  M within 25 minutes before plateauing.

5 control discs subjected to turbulent flow conditions were able to increase calcium ion and carbonate ion concentrations by  $4.4 \times 10^{-5}$  M within 20 minutes in the first flush, before plateauing. In the second and third flushes, calcium ion and carbonate ion concentrations increased by  $4.3 \times 10^{-5}$  M within 20 minutes before plateauing.

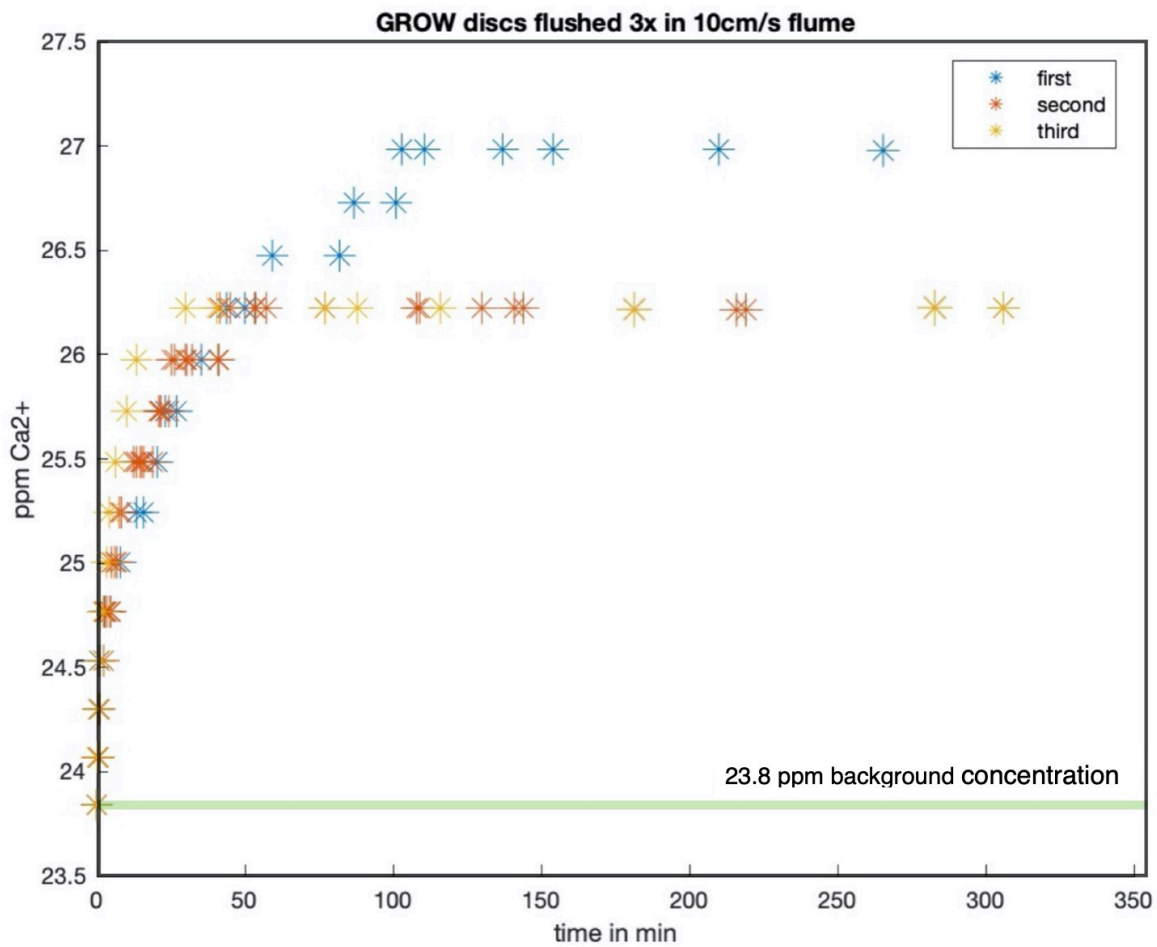


Figure 4.7: Plot of calcium ion concentration (ppm) against time (min) for 5 GROW discs that were subjected to three continuous runs in the flume at 10 cm/s water velocity. The instrument uncertainty is  $< 1$  ppm  $\text{Ca}^{2+}$ .

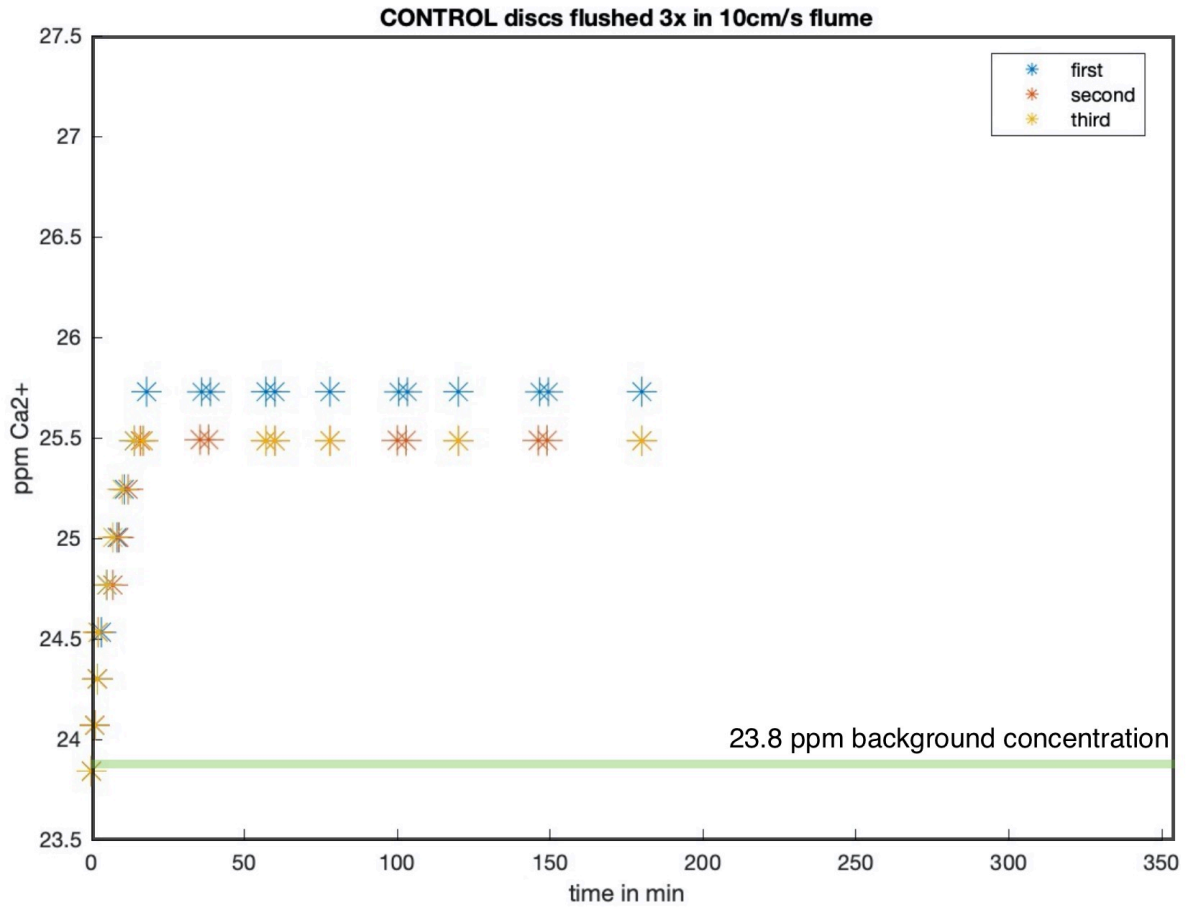


Figure 4.8: Plot of calcium ion concentration (ppm) against time (min) for 5 control discs that were subjected to three continuous runs in the flume at 10 cm/s water velocity. The instrument uncertainty is  $< 1$  ppm  $\text{Ca}^{2+}$ .

## 4.5 Material Testing

Table 4.10 summarizes results of material strength testing performed in an Instron compression machine on both ASTM-C39 standard test cylinders of each material and untreated discs of each material. Test cylinders and untreated discs were loaded in compression at a rate of 0.2 MPa/s. Five test cylinders of each material were tested, and three discs of each material were tested. The control test cylinders had an average compressive strength of 42.4 MPa (SD= 1.9 MPa), while GROW test cylinders had an average compressive strength of 40.51 MPa (SD= 0.97 MPa). The untreated control discs had an average compressive strength of 46.0 MPa (SD= 1.6 MPa), while the untreated GROW discs had an average compressive strength of 47.5 MPa (SD= 0.8 MPa). Material type had no significant effect on compressive strength of the test cylinders,  $t(8) = -1.8$ ,  $p = .12$ , or the untreated discs,  $t(4) = -0.3$ ,  $p = .79$ . Additional t-tests performed revealed no statistically significant differences in mean compressive strength of test cylinders and discs for control material ( $t(6) = -2.4$ ,  $p = .06$ ) and GROW material ( $t(6) = 1.8$ ,  $p = .13$ ), suggesting that the disc surface topography does not negatively impact material strength of the overall disc structure.

Table 4.11 summarizes results of material strength testing performed in an Instron compression machine and a rebound hammer on untreated discs of each material. Material type had no significant effect on rebound hammer measurements of compressive strength of the untreated discs,  $t(4) = -0.3$ ,  $p = .44$ . Testing method had no significant effect on compressive strength measurements of the untreated discs for both control ( $t(4) = 3.3$ ,  $p = .15$ ) and GROW ( $t(4) = -4.3$ ,  $p = .66$ ) materials, validating the use of rebound hammers as an in-situ material strength test.

Table 4.12 presents results of rebound hammer testing of discs after field deployment. Three out of five discs from each of the eight treatment groups was tested with the rebound hammer because of the labor-intensive surface preparation process. The three discs furthest from the bed in each treatment group was selected to avoid interference

from the effect of depth. Discs of both material types decreased in compressive strength after the first three months in the field, but subsequently increased in compressive strength with increasing submersion time. However, the discs did not return to the compressive strength of the original discs. T-tests confirm that neither material was stronger than the other at any of the submersion times tested.

Table 4.13 presents results of Instron compression machine testing of discs after field deployment. Only one disc from each of the eight treatment groups was tested with the Instron compression machine because of the labor-intensive surface preparation process. Discs of both material types decreased in compressive strength after the first three months in the field, and gradually increased in compressive strength with submersion time.

Figure 4.8 is a graphical representation of the compressive strength of GROW and control discs before treatment, after 90 days, 180 days, 330 days, and 420 days of treatment. The minimum compressive strength required of marine concrete is 35 MPa as designated by the American Concrete Institute; this value is marked on Figure 4.8 (“Guide for the Design and Construction of Fixed Offshore Concrete Structures” 1994).



Table 4.10: Compressive strength of test cylinders (of 3"x 6" standard size) and untreated discs as measured by an Instron compression machine. Test cylinders and untreated discs were loaded in compression at a rate of 0.2 MPa/s. Five test cylinders of each material were tested, and three discs of each material were tested. The average is the first number reported and the standard deviation is reported in brackets. The p-values are reported for independent paired t-tests performed between material types and between test cylinders vs. discs.

	<b>GROW Material (MPa)</b>	<b>Control Material (MPa)</b>	p-value for t-test between materials
<b>Test cylinders</b>	40.51 (0.97)	42.4 (1.9)	.12
<b>Discs</b>	47.5 (7.5)	46.0 (1.6)	.79
p-value for t-tests between cylinders and discs	.13	.06	

Table 4.11: Compressive strength of discs before field deployment as measured by a rebound hammer. Three test cylinders were tested. All forty field discs were tested prior to deployment. The average is the first number reported and the standard deviation is reported in brackets. The p-values are reported for independent paired t-tests performed between material types and between test cylinders vs. discs.

	<b>GROW Material (MPa)</b>	<b>Control Material (MPa)</b>	p-value for t-tests between materials
<b>Test cylinders</b>	45.0 (2.3)	43.0 (3.8)	.39
<b>Discs</b>	43.2 (6.7)	45.2 (7.7)	.44
p-value for t- tests between Rebound hammer and Instron	.66	.15	

Table 4.12: Compressive strength of discs after field deployment as measured by a rebound hammer. Three discs from each treatment group were tested. The three discs furthest from the bed in each treatment group was selected to avoid interference from the effect of depth. The average is the first number reported and the standard deviation is reported in brackets. The p-values are reported for independent paired t-tests performed between material types.

<b>Time deployed</b>	<b>GROW Discs (MPa)</b>	<b>Control Discs (MPa)</b>	<b>P</b>
<b>90 days</b>	19.9 (5.1)	21.1 (4.3)	.81
<b>180 days</b>	29.1 (1.8)	25.6 (3.2)	.25
<b>330 days</b>	32.2 (2.3)	31.7 (1.9)	.83
<b>420 days</b>	34.7 (0.7)	35.8 (3.9)	.68

Table 4.13: Compressive strength of discs after field deployment as measured by an Instron compression machine. Discs were dehydrated in a 200° C dehydration oven, then were loaded in compression at a rate of 0.2 MPa/s. One disc from each treatment group was tested. The disc furthest from the bed in each treatment group was selected to avoid interference from the effect of depth.

<b>Time deployed</b>	<b>GROW (MPa)</b>	<b>Control (MPa)</b>
<b>90 days</b>	26.6	19.8
<b>180 days</b>	24.6	30.8
<b>330 days</b>	27.6	33.4
<b>420 days</b>	30.7	37.7

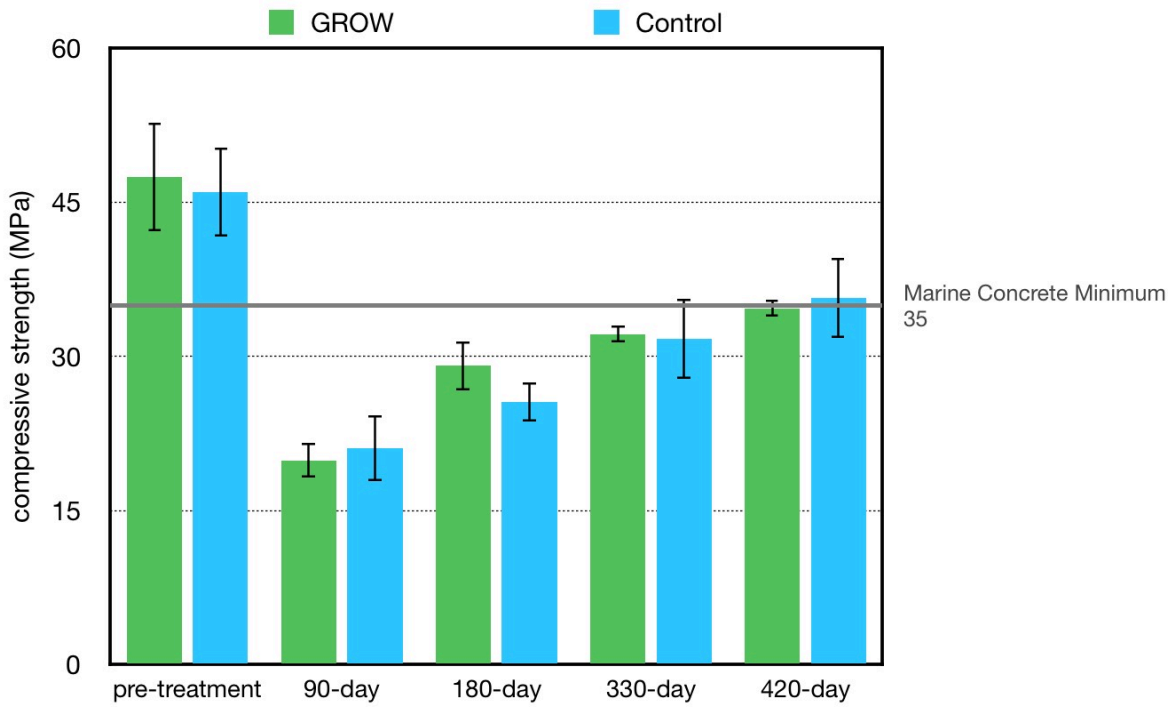


Figure 4.9: Average compressive strength (MPa) of GROW and control discs before field treatment and after 90, 180, 330, and 420 days of submersion in the field. Standard deviation is represented by the error bars. Compressive strength data represented here is from rebound hammer testing, although Instron compressive strength testing was also conducted to validate rebound hammer measurements. The minimum compressive strength required of marine concrete is 35 MPa as designated by the American Concrete Institute; the industry standard minimum is represented via a gray horizontal line.

# Chapter 5

## Discussion

The increasing frequency with which natural coastal habitats are replaced with concrete infrastructure has led to new design approaches which aim to enhance biodiversity and recruit ecosystem engineers (eg. Firth et al. 2014; Hanlon et al. 2018; Loke 2015). A limited number of studies have investigated the effect of CaCO<sub>3</sub>-enriched and/or ground oyster shell-enriched concrete formulas on marine recruitment (Hanlon et al. 2018; Perkol-Finkel and Sella 2014), and even fewer on material strength (Risinger 2012) and calcium and carbonate ion leaching (Green et al. 2013). Studies using concrete formulas which incorporated CaCO<sub>3</sub> and/or ground oyster shell have reported increased bivalve recruitment (Hanlon et al. 2018) as well as increased recruitment of other ecosystem engineer species such as serpulid worms, barnacles, and corals (Perkol-Finkel and Sella 2014). Risinger (2012) found that oyster recruitment resulted in a ten-fold increase in the flexural strength of submerged concrete structures. Here, the change in community composition and material strength over a 420-day period in response to the inclusion of CaCO<sub>3</sub> via ground oyster shells in the concrete substrate formula was tested, in addition to the leaching potential of enriched concrete.

Chemical cues from crushed mollusk shells are thought to be important determinants of community structure and dynamics because of their demonstrated ability to increase

larval recruitment, conspecific settlement, and heterospecific settlement (Hay 2009; Green et al. 2013; Vasquez et al. 2013; Browne and Zimmer 2001). Factors influencing the success of crushed mollusk shells as a settlement cue for mollusks include the amount of crushed shells provided and the species of shell used. For the oyster species *Crassostrea gigas* (Pacific oyster), studies have found that larval settlement is proportionate to the amount of crushed shell chips provided to larvae, regardless of shell species (Vasquez et al. 2013; Hay 2009). For the oyster species *C. gigas* and *Crassostrea virginica* (American oyster), larvae display greater settlement on conspecific shells rather than heterospecific shells (Vasquez et al. 2013; Crisp 1967; Pawlik 1992). The inclusion of CaCO<sub>3</sub> via oyster material in the concrete substrate formula was expected to influence community structure and enhance bivalve recruitment; I hypothesized that discs constructed of the GROW material would release a chemical cue in the form of calcium ions, carbonate ions, and oyster shell glycoproteins that would 1) result in a different community makeup 2) increase recruitment of mollusks in general and oysters specifically.

The GROW material had minimal effect on the recruited communities as a whole, although two key differences were observed: 1) higher counts of mussels and larger mussels were observed on GROW discs when mussels appeared during the 330-day and 420-day retrievals (Table 4.6), and 2) GROW discs had higher percent coverage of calcareous recruitment on the innermost surface throughout all submersion times. The GROW discs and control discs displayed highly similar communities (> 82% similarity) across all submersion times (Figure 4.2, Table 4.7), suggesting that CaCO<sub>3</sub> in the concrete formula had minimal effect on the community. The dissimilarity between community makeup on GROW discs and control discs was associated with the higher percent coverage of barnacles on GROW discs in the 90-day retrieval (21% contribution to dissimilarity, Table 4.7), suggesting that the GROW formula was more effective in recruiting barnacles during this 90-day window. Barnacles are considered ecosystem engineers (Perkol-Sella and Finkel 2014) because they increase substrata heterogeneity,

which in turn increases surface area for biofilm or larval attachment and provides protection from desiccation (Mrowicki et al. 2014). On the other hand, barnacles also directly compete with other bivalves for nutrients and space, particularly oysters (Mrowicki et al. 2014). The recruitment of barnacles during later submersion times and its impact on material strength is discussed later in this section.

In New England, the blue mussel *Mytilus edulis* typically peaks in reproduction during the months of May and June (Carrington 2002). When mussels appeared on the discs retrieved at 330-day and 420-day (retrieved July 8<sup>th</sup>, 2020 and October 6<sup>th</sup>, 2020 respectively), higher counts of mussels were observed on GROW discs (Table 4.6). Mussels of various sizes were observed on the discs, ranging from < 1cm to 4cm in length (Table 4.6). On discs from the 330-day retrieval, only < 1 cm long mussels were observed on both material types (Table 4.6). GROW discs from the 420-day retrieval had on average 6.4 (SD= 1.0) mussels per disc, with 3 mussels of 4 cm length (Table 4.6). Control discs from the 420-day retrieval had only 1.4 (SD= 1.0) mussels per disc, and only 1 mussel of 4 cm length (Table 4.6). GROW discs demonstrated greater success in recruiting more and larger mussels. Bivalves have been shown to settle in response to heterospecific cues from the same family (Vasquez et al. 2013), suggesting that the inclusion of oyster material in the GROW concrete formula could be a viable method for increasing recruitment of mollusks. Other factors, in addition to presence of a chemical cue, could have influenced mussel recruitment to the discs, including local hydrodynamics and the presence of live conspecifics. Bivalve larvae often select local low shear areas on the substrate for attachment (Mullineaux and Butman 1991; Whitman and Reidenbach 2012). The mussels recruited to our discs were mainly attached to the discs in the hemispherical cavities; I hypothesize that the cavities provided pockets in which velocity and turbulence are reduced and mussel larvae could attach without being dislodged. The presence of live conspecifics is considered to be another important driver of mollusk larval settlement (Crisp 1967); live conspecifics are able to release chemical cues that induce high rates of larval settlement. In addition to the chemical cue of

CaCO<sub>3</sub> in the concrete formula and the low-shear cavities, larger adult mussels were possibly involved in conspecific recruitment of mussel larvae to our discs. Since recruitment was only observed at discrete points in time and not continuously, it is not possible to conclude whether mussels were involved in conspecific recruitment or if mussels present at 330 days just grew into larger adults. Although the data suggest that the addition of chemical cues to concrete formulas may increase mollusk recruitment, the importance of chemical cues relative to live conspecifics and surface topography remains unclear, as does the interplay between these three factors.

Throughout all submersion times, GROW discs had higher percent coverage of calcareous recruitment on the innermost disc surface (Table 4.5). Calcareous recruitment on the innermost disc surface consisted of barnacles and *C. fornicata* (common slipper shell). Due to the strong correlation between material type and calcareous recruitment, it is hypothesized that increased calcium and carbonate ion leaching from the GROW material provided both the recruitment cue and the building blocks necessary for shell precipitation of barnacles and *C. fornicata*.

The concentration of calcium ions and carbonate ions available in the flow around the concrete substrate must be sufficient in order for bivalves to precipitate shells (Green et al. 2013). The thermodynamic tendency of shell precipitation is represented by the aragonite saturation state,

$$\Omega_{\text{aragonite}} = \frac{[\text{Ca}^{2+}] [\text{CO}_3^{2-}]}{K'_{sp}}$$

Calcium ion and carbonate ion concentrations above the equilibrium value of  $6 \times 10^{-5}$  to  $9 \times 10^{-5}$  M are required for shell precipitation. GROW discs studied in low velocity (10cm/s) but fully turbulent conditions in the flume demonstrated that five discs were able to increase calcium ion and carbonate ion concentrations by  $8.7 \times 10^{-5}$  M within 100 minutes. This amount of ion leaching would satisfy the ion concentration requirements for shell precipitation even in deionized water. Control discs were able to increase

calcium ion and carbonate ion concentrations by  $4.4 \times 10^{-5}$  M before plateauing. Although GROW discs leached higher concentrations of calcium and carbonate ions, discs of both material types demonstrated the ability to provide continued leaching of ions; suggesting that the  $\text{CaCO}_3$  component is well mixed in GROW discs and that porosity is consistent throughout both GROW and control discs. In turbulent, well-mixed conditions, in which the diffusive transport across the diffusive sub-layer controls the flux from the substrate, ion concentration in the well-mixed water volume is  $C = C_{eq}(1 - e^{-kt})$ , in which  $k = \left[ \frac{D_m A}{V \delta_c} \right]$ . If the  $\text{CaCO}_3$  component is well-mixed in the concrete formula,  $C_{eq}$  remains constant even when top layers of the concrete substrate have dissolved in the flow, and the substrate is able to provide continued leaching of ions to the same steady-state concentration, as long as the flow conditions remain constant. Ion leaching from a porous substrate like the discs involves diffusion in the pores of the substrate as well, and the porosity influences the diffusion coefficient  $D_m$ . Since the discs were able to provide continued leaching of ions to the same steady-state concentration, I hypothesize that porosity and thus the diffusion coefficient remains consistent throughout the disc material. I hypothesize that early colonizers, barnacles and *C. fornicata*, were able to make use of available calcium and carbonate ions, and continue to expand their coverage on the innermost layer of growth directly atop the concrete substrate by growing in size. This implies that the GROW formula initially promotes the recruitment of calcareous species larvae, and then supports the health and survival of adults. Although invasive ascidians were very competitive for surface area, it is possible that barnacle and *C. fornicata* grew in population sizes in addition to individual sizes, via live conspecific cues instead of ion leaching, as invasive ascidians dominated the surface and obstructed ion leaching. Given the density of the ascidian colonies on the disc surfaces, conspecific recruitment of barnacles and *C. fornicata* seems unlikely; it is more likely that both species experienced early colonization and continued growth.



The effect of seashell enrichment on early concrete material strength is well studied, but the effect on durability (changes in material strength with time or exposure) is not. When seashells are used as a partial aggregate substitute in concrete formulation, the compressive strength is typically lower than standard concrete formulations (Mo et al. 2018; Tayeh et al. 2019). Some studies have found that seashells incorporated as finer aggregates or  $\text{CaCO}_3$  powder have less of a negative impact on compressive strength, tensile strength, and/or flexural strength, and some have even found that certain ratios of replacement via ground shells can increase material strength (Tayeh et al. 2019; Peceño et al. 2019). Tayeh (2019) found that compressive strength is optimized when the cement component of concrete is replaced by 10% periwinkle seashell ash, 15% oyster seashell ash, or 20% snail seashell ash by weight. The GROW and control formulas tested did not have different compressive strengths, both prior to submersion and after submersion. Although compressive strength did vary with submersion time, it did not vary with inclusion of  $\text{CaCO}_3$  in the formula. Initial submersion greatly impacted material strength of both GROW and control formulas, with compressive strength reducing to around half its original value after 90 days of submersion in the field. After the initial decrease, compressive strength increased with submersion time in the field, but never recovered to its original strength. Barnacles and *Crepidula fornicata* (Common slipper shell) increased in substrate surface coverage with submersion time (Table 4.5); I hypothesize that increased compressive strength with submersion time was related to increased calcareous recruitment of barnacles and *C. fornicata*. Risinger (2012) previously demonstrated that concrete populated by adult oysters has higher compressive and flexural strengths when tested against non-populated concrete. Studies on the compressive strength of bivalves alone (not on concrete) report values between 60 MPa and 150 MPa (Taylor and Layman 1972; Yang et al. 2011; Karande and Udhayakumar 1989), which are higher than the 35 MPa typically required of marine concrete (“Guide for the Design and Construction of Fixed Offshore Concrete Structures” 1994). The presence of bivalves on the surface of marine concrete have the potential to

strengthen the concrete structure and also protect it from degradation from wave energy, freeze-thaw, or burrowing species. (Note that increased barnacle and *C. fornicata* coverage is not represented in percent coverage data as percent coverage was analyzed from the top surface layer of growth, not from the innermost layer of growth directly atop the concrete substrate).

The presence of oyster shell glycoproteins in the GROW formula was expected to recruit oysters specifically in addition to mollusks generally, as oysters are typically responsive to conspecific shells as a recruitment cue (Crisp 1967, Vasquez et al. 2013), and because oysters have been observed in the surrounding tidal flats in Savin Hill Cove, near Fallon Pier (Francik 2012, Lockwood, personal communication, 2020). The American oyster *Crassostrea virginica* is the primary oyster species in Massachusetts waters (Bowen, n.d.). *C. virginica* spawns once water temperatures reach 15 to 16° C, typically in late May or early June in Boston (Nelson 1928, NOAA, n.d.). Assuming nearby oyster populations are in good reproductive health, oyster larvae would have been present in June. If larval settlement and subsequent growth had been successful, small 1 to 2-month-old oysters would have been observed during the 330-day recruitment on July 8<sup>th</sup>, 2020, or 2 to 5-month-old oysters would have been observed during the 420-day recruitment on October 6<sup>th</sup>, 2020. However, no oysters were recruited to either GROW or control discs. Oyster settlement cue via GGR protein is shown to be only effective in the mm-cm range of the water column above the substrate, when the substrate surfaces are uncovered (Gross, Werner, and Eckman 1992; Turner et al. 1994; Browne and Zimmer 2001). The surfaces of both GROW and control discs were completely colonized within 90 days of submersion, mainly by barnacles and hydroids. It is possible that nearby oyster populations were not large or healthy enough to spawn sufficient numbers of larvae to reach and settle on the deployed discs, although this possibility is unlikely given the recorded observations of oyster populations in Savin Hill Cove (Francik 2012). I hypothesize that colonization of the disc surface by other species obstructed the surface and reduced leaching of recruitment cues before oyster larvae from the summer

spawning season had the opportunity to encounter the cues. Concentrations of recruitment cues were possibly not high enough in the flow surrounding the discs to induce settling of oyster larvae when oyster larvae became present at high numbers in the summer, due to surface colonization by other species. To our knowledge, the effect of surface colonization on the leaching of chemical cues from a substrate has not yet been investigated.

Certain resident species (species already present on substrates) can reduce oyster larval settlement (Osman, Whitlach, and Zajac 1989). The main resident species observed on both GROW and control discs included common sessile invertebrates such as barnacles, ascidians, and bryozoans. Most barnacle, ascidian, and bryozoan species reduce oyster larvae attachment by covering substrate available for attachment, and reduce post-attachment oyster survivorship by competing for planktonic food (Osman 1989). Barnacles and the ascidians *Ascidiella aspersa*, *Botrylloides violaceus*, and *Didemnum* sp. dominated disc surfaces after all four submergence times, and likely contributed to the failure of oyster larvae to attach and/or survive post-attachment during the summer months. Colonization of the disc surfaces by these four species also altered the surface topography of the discs. Barnacles and ascidians filled in the hemispherical cavities, reducing the number of low-velocity pockets that induce larval attachment. *Styela clava*, a solitary ascidian that was observed to grow in both percent coverage and size of individual organisms with submersion time, is a predator of oyster larvae (Osman 1989). The successful colonization and growth of *S. clava* was another likely factor in the failure of oysters to emerge in our disc communities.

Although the community structure of the deployed discs did not vary more than 20% with material type (Table 4.7), community structure did vary with submersion time. Figure 4.2 provides a visual representation of the time-dependent effects on community makeup. Some species, notably *Didemnum* sp. and *S. clava*, grew in surface coverage with time. Other species, such as hydroids, tubes, *A. aspersa*, and *B. violaceus*

experienced peak coverage during a specific season (Figure 4.2). Species that experience peak coverage during a specific season are considered to be opportunistic species: they can rapidly form dense single-species assemblages that dominate competitive interactions, but also experience intraspecific competition that leads to rapid die-off (Dorsey 1982; Osman 1977; Jackson 1977). This rapid growth and die-off phenomenon is referred to as a boom-bust cycle. Hydroids experienced a boom at 90 days, followed immediately by a bust at 180 days. Tubes experienced a slower boom, peaking at 180 days, followed immediately by a bust at 330 days. The ascidians *A. aspersa* and *B. violaceus* appeared at 180 days but peaked at 330 days, followed by a bust at 420 days, when *Didemnum* sp. outcompeted both of them. The results from SIMPER analysis reinforced the seasonal boom-bust patterns observed on both GROW and control discs (Table 4.7, 4.8). The species that was the main contributor to community structure dissimilarity between submersion times evolved from hydroids, to tubes, to *Didemnum* sp. as the seasons progressed. Percent contribution to dissimilarity by the main contributing species also increased as submersion time increased, suggesting that as discs were submerged longer, the disc surface became more dominated by a single species (*Didemnum* sp.), making the surface homogenous and less diverse.

*S. clava*, *A. aspersa*, *B. violaceus*, and *Didemnum* sp. are all non-native ascidian species that began invading New England waters in the 1970s to 1980s (Osman 1999). In areas where local resident sessile diversity is low, invasive ascidians are able to rapidly dominate communities and coastal substrate surfaces. A 2018 survey of New England marinas found that the most frequently observed introduced invertebrate species were *Botrylloides violaceus*, *Botryllus schlosseri*, *Caprella mutica*, *Styela clava*, *Asciidiella aspersa*, *Ciona intestinalis*, *Didemnum vexillum*, and *Tricellaria inopinata* (Kennedy et al. 2020). Certain ascidian species have microscopic spicules made of calcium carbonate, although calcium carbonate accounts for much less of their overall anatomy than mollusk species. *Didemnum vexillum* is composed of 0.004 to 0.04% calcium carbonate by weight only (Reinhardt, Gallagher, and Stefaniak 2012). The main predators of *S.*

*clava* and *A. aspersa* are small snail species and the fish *Tautoglabrus adspersus*, although *S. clava* is able to escape predation more easily than native species (Osman 1999). The *Didemnum* sp. recruited to the discs is most likely *Didemnum vexillum*, which has been observed to have great presence in New England waters since the 1980s (Kennedy et al. 2020).

The colonial ascidian *Didemnum* sp. grows rapidly in the summer months, and typically declines in health and population size starting in October when water temperatures begin to fall. *Didemnum* sp. has no predators in New England waters, and thus tends to rapidly overgrow other species, often enveloping mussels, oysters, sea scallops, and other bivalves (Valentine et al. 2007). In 2018, *Didemnum vexillum*, was observed at higher frequencies than ever before in New England marinas (Kennedy et al. 2020). Auker and Oviatt (2008) have suggested that higher boat and mooring presence is correlated with higher *Didemnum* sp. presence. Fletcher, Atalah, and Forrest (2018) found that summer or autumn deployment of substrates leads to greatest *Didemnum vexillum* colony coverage, with peak coverage occurring in the following summer or autumn after an initial lag in coverage. The same *Didemnum* sp. seasonal recruitment pattern was observed in our discs: the discs from the 330-day and 420-day retrievals on July 8<sup>th</sup>, 2020 and October 6<sup>th</sup>, 2020 respectively showed an increase in percent coverage of *Didemnum* sp. A spring or winter deployment of concrete substrates may be a worthwhile strategy for avoiding *Didemnum* sp. overgrowth during future deployments in areas where *Didemnum* sp. is a known invader or where there is high boating and mooring activity.

# Chapter 6

## Summary

Although the inclusion of  $\text{CaCO}_3$  via oyster material in the GROW concrete formula had minimal effect on the composition and abundance of recruited communities as a whole, we observed higher counts of mussels and larger mussels on GROW discs, and also higher percent coverage of heavily calcified organisms such as barnacles on GROW discs. The addition of  $\text{CaCO}_3$  as a chemical cue in concrete may increase mollusk and general calcareous recruitment through the leaching of calcium and carbonate ions as a recruitment cue, or as building blocks for shell precipitation. However, chemical cues are not the only important factor in mollusk recruitment, as the presence of live conspecifics and low-shear surface pockets are also hypothesized to increase recruitment of mollusks (Crisp 1967, Vasquez et al. 2013, Mullineaux and Butman 1991). The presence of larger mussels on GROW discs from the 420-day retrieval was encouraging, as it implied that the GROW discs support the health and survival of adult mollusks. The leaching potential calcium and carbonate ions from GROW discs was demonstrated in turbulent flume conditions to be more than adequate for shell precipitation. GROW material strength and durability were not significantly different to standard marine concrete. Material strength of both materials did initially decrease after submersion, but increased with submersion time without ever reaching its original material strength value. I hypothesize that increased calcareous species surface coverage by barnacles and common

slipper shells increased concrete compressive strength. No oysters were recruited to any discs, most likely because the colonization of the disc surface by invasive ascidians reduced available surface area for settlement and also reduced the leaching of recruitment cues before oyster larvae from the summer spawning season had the opportunity to encounter the cues. To our knowledge, the effect of surface colonization on the leaching of chemical cues from a substrate has not yet been investigated, so this represents an area for future study. Community structure varied more with submersion time than with material type. Community structure varied in time following boom-bust cycles, where the invasive ascidians *S. clava*, *A. aspersa*, *B. violaceous*, and *Didemnum sp.* competed for surface coverage. Future deployments in areas where invasive ascidians are present should carefully consider the timing of deployment. A spring deployment of CaCO<sub>3</sub> enriched concrete is suggested, so that the oyster spawning occurs before the arrival of invasive species. This will likely provide oyster larvae from the summer spawning season increased opportunities to encounter chemical cues and greater surface area for attachment without interference from ascidians colonizing the surfaces and potentially limiting leaching of chemical cues.

# Sources

- Airoidi, Laura. 2003. "The Effects of Sedimentation on Rocky Coast Assemblages." *Oceanography and Marine Biology Annual Review* 41: 161–236.
- Auker, L. A., and C. A. Oviatt. 2008. "Factors Influencing the Recruitment and Abundance of *Didemnum* in Narragansett Bay, Rhode Island." *ICES Journal of Marine Science* 65 (5): 765–69.
- Barbier, E. B., S. D. Hacker, C. Kennedy, E. W. Koch, A. C. Stier, and B. R. Silliman. 2011. "The Value of Estuarine and Coastal Ecosystem Services." *Ecological Monographs* 81 (2): 169–93. <https://doi.org/10.1890/10-1510.1>.
- Barker, S., and A. Ridgwell. 2012. "Ocean Acidification." *Nature Education Knowledge* 3 (10): 21.
- Barragan, J. M., and M. de Andres. 2015. "Analysis and Trends of the World's Coastal Cities and Agglomerations." *Ocean and Coastal Management* 114.
- Bartol, I., R. Mann, and M. Luckenbach. 1999. "Growth and Mortality of Oysters (*Crassostrea Virginica*) on Constructed Intertidal Reefs: Effects of Tidal Height and Substrate Level." *Journal of Experimental Marine Biology and Ecology* 237 (2): 157–84.
- Bell, R., R. Buchsbaum, C. Roman, and M. Chandler. 2005. "Inventory of Intertidal Marine Habitats, Boston Harbor Islands National Park Area." *Northeastern Naturalist* 12 (sp3): 169–200. [https://doi.org/10.1656/1092-6194\(2005\)12\[169:IOIMHB\]2.0.CO;2](https://doi.org/10.1656/1092-6194(2005)12[169:IOIMHB]2.0.CO;2).
- Bishop, M. J., M. Mayer-Pinto, L. Airoidi, L. B. Firth, R. L. Morris, L. H. L. Loke, S. J. Hawkins, et al. 2017. "Effects of Ocean Sprawl on Ecological Connectivity: Impacts and Solutions." *Journal of Experimental Marine Biology and Ecology* 492 (July): 7–30. <https://doi.org/10.1016/j.jembe.2017.01.021>.
- Boyle, D. 2020. "Oystering in Connecticut, from Colonial Times to the 21st Century." *ConnecticutHistory.Org* (blog). August 27, 2020. <https://connecticuthistory.org/oystering-in-connecticut-from-colonial-times-to-today/>.
- Browne, K. A., and R. K. Zimmer. 2001. "Controlled Field Release of a Waterborne Chemical Signal Stimulates Planktonic Larvae to Settle." *The Biological Bulletin* 200 (1): 87–91. <https://doi.org/10.2307/1543088>.
- Carde, C, R Francois, and J Torrenti. 1996. "Leaching of Both Calcium Hydroxide and C-S-H from Cement Paste: Modeling the Mechanical Behavior." *Cement and Concrete Research* 26 (8): 1257–68.
- Carrington, E. 2002. "Seasonal Variation in the Attachment Strength of Blue Mussels: Causes and Consequences." *Limnology and Oceanography* 47 (6): 1723–33.
- Chapman, M. G. 2003. "Paucity of Mobile Species on Constructed Seawalls: Effects of Urbanization on Biodiversity." *Marine Ecology Progress Series* 264: 21–29. <https://doi.org/10.3354/meps264021>.



- Chapman, M.G., and Mark Anthony Browne. 2014. *Mitigating against the Loss of Species by Adding Artificial Intertidal Pools to Existing Seawalls*. Vol. 497. <https://doi.org/10.3354/meps10596>.
- Clarke, K.R. 1993. "Non-Parametric Multivariate Analyses of Changes in Community Structure." *Australian Journal of Ecology* 18 (1): 117–43.
- Crisp, D. J. 1967. "Chemical Factors Inducing Settlement in *Crassostrea Virginica* (Gmelin)." *The Journal of Animal Ecology* 36 (2): 329. <https://doi.org/10.2307/2916>.
- Dorsey, J. H. 1982. "Intertidal Community Offshore from the Werribee Sewage-Treatment Farm: An Opportunistic Infaunal Assemblage." *Australian Journal of Marine and Freshwater Research* 33 (1): 45–54.
- Elder, J. W. 1959. "The Dispersion of Marked Fluid in Turbulent Shear Flow." *Journal of Fluid Mechanics* 5 (4): 544–60. <https://doi.org/10.1017/S0022112059000374>.
- Elzinga, C. L, D. W. Salzer, and J. W. Willoughby. 1998. *Measuring and Monitoring Plant Populations*. Bureau of Land Management Technical Reference 1730-1.
- EPA. 2020a. "Aquatic Nuisance Species (ANS)." *United States Environmental Protection Agency* (blog). 2020. <https://www.epa.gov/vessels-marinas-and-ports>.
- EPA. 2020b. "Green Infrastructure Design and Implementation." *United States Environmental Protection Agency* (blog). 2020. <https://www.epa.gov/green-infrastructure/green-infrastructure-design-and-implementation>.
- Firth, L.B., R.C. Thompson, K. Bohn, M. Abbiati, L. Airoidi, T.J. Bouma, F. Bozzeda, et al. 2014. "Between a Rock and a Hard Place: Environmental and Engineering Considerations When Designing Coastal Defence Structures." *Coastal Engineering* 87 (May): 122–35. <https://doi.org/10.1016/j.coastaleng.2013.10.015>.
- Fletcher, L. M., J. Atalah, and B. M. Forrest. 2018. "Effect of Substrate Deployment Timing and Reproductive Strategy on Patterns in Invasiveness of the Colonial Ascidian *Didemnum Vexillum*." *Marine Environmental Research* 141 (October): 109–18.
- Francik, A. 2012. "Green Boston Harbor Project (GBH), Community Environmental Stewardship: Applied Research, Education and Outreach." *ScholarWorks at UMass Boston*.
- Grabowski, J. H., R. D. Brumbaugh, R. F. Conrad, A. G. Keeler, J. J. Opaluch, C. H. Peteron, M. F. Piehler, S. P. Powers, and A. R. Smyth. 2012. "Economic Valuation of Ecosystem Services Provided by Oyster Reefs."
- Green, A. A., G. C. Waldbusser, L. Hubazc, E. Cathcart, and J. Hall. 2013. "Carbonate Mineral Saturation State as the Recruitment Cue for Settling Bivalves in Marine Muds." *Estuaries and Coasts* 36 (1): 18–27. <https://doi.org/10.1007/s12237-012-9549-0>.
- Gross, T. F., F. E. Werner, and J. E. Eckman. 1992. "Numerical Modeling of Larval Settlement in Turbulent Bottom Boundary Layers." *Journal of Marine Research* 50 (4): 611–42. <https://doi.org/10.1357/002224092784797575>.
- "Guide for the Design and Construction of Fixed Offshore Concrete Structures." 1994. *American Concrete Institute 357R-84*.
- Gutiérrez, Jorge L., Clive G. Jones, David L. Strayer, and Oscar O. Iribarne. 2003. "Mollusks as Ecosystem Engineers: The Role of Shell Production in Aquatic Habitats." *Oikos* 101 (1): 79–90. <https://doi.org/10.1034/j.1600-0706.2003.12322.x>.
- Hanlon, Nadine, Louise B. Firth, and Antony M. Knights. 2018. "Time-Dependent Effects of Orientation, Heterogeneity and Composition Determines Benthic Biological Community

- Recruitment Patterns on Subtidal Artificial Structures.” *Ecological Engineering* 122 (October): 219–28. <https://doi.org/10.1016/j.ecoleng.2018.08.013>.
- Hay, M. E. 2009. “Marine Chemical Ecology: Chemical Signals and Cues Structure Marine Populations, Communities, and Ecosystems.” *Annual Review of Marine Science* 1 (1): 193–212. <https://doi.org/10.1146/annurev.marine.010908.163708>.
- Heukamp, F. H. 2003. “Chemomechanics of Calcium Leaching of Cement-Based Materials at Different Scales: The Role of CH-Dissolution and C-S-H-Degradation on Strength and Durability Performance of Materials and Structures.” Doctor of Philosophy, Massachusetts Institute of Technology.
- Jackson, J. B. C. 1977. “Competition on Marine Hard Substrata: The Adaptive Significance of Solitary and Colonial Strategies.” *The American Naturalist* 111 (1980).
- Karande, A. A., and M. Udhayakumar. 1989. “Shell Structure and Shell Strength in Cirripedes.” *Proceedings: Animal Sciences* 98 (4): 223–31. <https://doi.org/10.1007/BF03179403>.
- Kays, W., and M. Crawford. 1993. *Convective Heat and Mass Transfer*. 3rd ed. McGraw-Hill, New York.
- Kennedy, C., A.L. Pappal, C. Bastidas, and J.T. Carlton, A.A. David, J.A. Dijkstra, S. Duffey, J. Gibson, S.P. Grady, L.A. Green, Gavrielidis, L.G. Harris, N.-V. Hobbs, A. Mauk, M. McCuller, C. Neefus, B. O’Brien, K. Osborne, J. Pederson, J. Robidoux, M. Tyler, and K. Van. 2020. “Report on the 2018 Rapid Assessment Survey of Introduced, Cryptogenic, and Native Marine Species at New England Marinas: Massachusetts to Maine.” *Commonwealth of Massachusetts, Executive Office of Energy and Environmental Affairs, Office of Coastal Zone Management, Boston, MA.*, 34.
- Ko, H., C. Ratri, K. Kim, Y. Jung, G. Tae, and K. Shin. 2020. “Formulation of Sugar/Hydrogel Inks for Rapid Thermal Response 4D Architectures with Sugar-Derived Macropores.” *Nature Scientific Reports*, 11. <https://doi.org/10.1038/s41598-020-64457-8>.
- Lackovic, R. 2019. “A History of Oysters in Maine (1600s-1970s).” *Darling Marine Center Historical Documents* 22. [https://digitalcommons.library.umaine.edu/dmc\\_documents/22](https://digitalcommons.library.umaine.edu/dmc_documents/22).
- Lagerblad, B. 2007. *Leaching Performance of Concrete Based on Studies of Samples from Old Concrete Constructions*. The University of Michigan.
- Lau, Y. L., and D. Liu. 1993. “Effect of Flow Rate on Biofilm Accumulation in Open Channels.” *Water Research* 27 (3): 335–60.
- Lindsey, R. 2020. “Climate Change: Atmospheric Carbon Dioxide.” *NOAA Climate.Gov* (blog). August 14, 2020. <https://www.climate.gov/news-features/understanding-climate>.
- Loke, L. H. L. 2015. “ENHANCING BIODIVERSITY ON TROPICAL SEAWALLS: HOW HABITAT COMPLEXITY AND FRAGMENTATION REGULATE INTERTIDAL COMMUNITIES.” PhD, Singapore: National University of Singapore.
- Marin, F., and G. Luquet. 2004. “Molluscan Shell Proteins.” *Comptes Rendus Palevol* 3 (6–7): 469–92. <https://doi.org/10.1016/j.crpv.2004.07.009>.
- Mehta, P. K. 1986. *Concrete. Structure, Properties, and Materials*. Prentice-Hall.
- Mo, K. H., U. J. Alengaram, M. K. Jumaat, S. C. Lee, W. I Goh, and C. W. Yuen. 2018. “Recycling of Seashell Waste in Concrete: A Review.” *Construction and Building Materials* 162 (February): 751–64. <https://doi.org/10.1016/j.conbuildmat.2017.12.009>.
- Mrowicki, R. J., C. A. Maggs, and N. E. O’Connor. 2014. “Does Wave Exposure Determine the Interactive Effects of Losing Key Grazers and Ecosystem Engineers?” *Journal of Experimental Marine Biology and Ecology* 461: 416–24.

- Mullineaux, L. S., and C. A. Butman. 1991. "Initial Contact, Exploration and Attachment of Barnacle (*Balanus Amphitrite*) Cyprids Settling in Flow." *Marine Biology* 110: 93–103.
- Neal, A. L., and A. Yule. 1994. "The Tenacity of *Elminius Modestus* and *Balanus Perforatus* Cyprids to Bacterial Films Grown under Different Shear Regimes." *Journal of the Marine Biological Association of the UK* 74 (01): 251–57.
- Osman, R. W. 1977. "The Establishment and Development of a Marine Epifaunal Community." *Ecological Monographs* 47 (1): 37–63.
- Osman, R. W., and R. B. Whitlach. 1999. "Ecological Interactions of Invading Ascidians within Epifaunal Communities of Southern New England." In , edited by J. Pederson. MIT Sea Grant College Program. MITSG Center for Coastal Resources, MIT, Cambridge, MA.
- Osman, R. W., R. B. Whitlach, and R. N. Zajac. 1989. "Effects of Resident Species on Recruitment into a Community: Larval Settlement versus Post-Settlement Mortality in the Oyster *Crassostrea Virginica*." *Marine Ecology Progress Series* 54 (June): 61–73.
- Pawlik, J. R. 1992. "Chemical Ecology of the Settlement of Benthic Marine Invertebrates." *Oceanography and Marine Biology Annual Review* 30: 273–335.
- Peceño, B., C. Arenas, B. Alonso-Fariñas, and C. Leiva. 2019. "Substitution of Coarse Aggregates with Mollusk-Shell Waste in Acoustic-Absorbing Concrete." *Journal of Materials in Civil Engineering* 31 (6): 04019077.  
[https://doi.org/10.1061/\(ASCE\)MT.1943-5533.0002719](https://doi.org/10.1061/(ASCE)MT.1943-5533.0002719).
- Perkol-Finkel, Shimrit, and Ido Sella. 2014. *Ecologically Active Concrete for Coastal and Marine Infrastructure: Innovative Matrices and Designs*.  
<https://doi.org/10.1680/fsts597571139>.
- Rees, S. E., N. L. Foster, O. Langmead, S. Pittman, and D. E. Johnson. 2018. "Defining the Qualitative Elements of Aichi Biodiversity Target 11 with Regard to the Marine and Coastal Environment in Order to Strengthen Global Efforts for Marine Biodiversity Conservation Outlined in the United Nations Sustainable Development Goal 14." *Marine Policy* 93 (July): 241–50. <https://doi.org/10.1016/j.marpol.2017.05.016>.
- Reinhardt, J., K. L. Gallagher, and L. Stefaniak. 2012. "Material Properties of *Didemnum Vexillum* and Prediction of Tendril Fragmentation." *Marine Biology* 159 (12).
- Risinger, Jon David. 2012. "Biologically Dominated Engineered Coastal Breakwaters." PhD, Louisiana State University.
- Secchi, E., A. Vitale, G.L. Mino, V. Kantsler, L. Eberl, R. Rusconi, and R. Stocker. 2020. "The Effect of Flow on Swimming Bacteria Controls the Initial Colonization of Curved Surfaces." *Nature Communications* 11 (June).
- Suprenant, B. 1991. "Designing Concrete for Exposure to Seawater." *The Aberdeen Group Publication #C910873*.
- Tan, Y Q, J V Smith, C Q Li, and J Dauth. 2017. "Calcium Leaching of a Concrete Tunnel Lining under Aggressive Groundwater Conditions," 6.
- "Tanaid." 2009. *Encyclopaedia Britannica* (blog). August 2009.  
<https://www.britannica.com/animal/tanaid>.
- Tayeh, B. A., M. W. Hasaniyah, A. M. Zeyad, and M. O. Yusuf. 2019. "Properties of Concrete Containing Recycled Seashells as Cement Partial Replacement: A Review." *Journal of Cleaner Production* 237 (November): 117723.  
<https://doi.org/10.1016/j.jclepro.2019.117723>.
- Taylor, J. D., and M. Layman. 1972. "The Mechanical Properties of Bivalve (Mollusca) Shell Structures." *Paleontology*, January.

- Tibbetts, J. 2002. "Coastal Cities: Living on the Edge." *Environmental Health Perspectives* 110 (11): A674–81.
- Turner, E. J., R. K. Zimmer-Faust, M. A. Palmer, M. Luckenbach, and N. D. Pentchef. 1994. "Settlement of Oyster ( *Crassostrea Virginica* ) Larvae: Effects of Water Flow and a Water-Soluble Chemical Cue." *Limnology and Oceanography* 39 (7): 1579–93. <https://doi.org/10.4319/lo.1994.39.7.1579>.
- Valentine, P. C., M. R. Carman, D. S. Blackwood, and E. J. Heffron. 2007. "Ecological Observations on the Colonial Ascidian *Didemnum* Sp. in a New England Tide Pool Habitat." *Journal of Experimental Marine Biology and Ecology* 342 (1): 109–21.
- Vasquez, H. E., K. Hashimoto, A. Yoshida, K. Hara, C. C. Imai, H. Kitamura, and C. G. Satuito. 2013. "A Glycoprotein in Shells of Conspecifics Induces Larval Settlement of the Pacific Oyster *Crassostrea Gigas*." Edited by T. Harder. *PLoS ONE* 8 (12): e82358. <https://doi.org/10.1371/journal.pone.0082358>.
- Waldbusser, G. G., R. A. Steenson, and M. A. Green. 2011. "Oyster Shell Dissolution Rates in Estuarine Waters: Effects of PH and Shell Legacy." *Journal of Shellfish Research* 30 (3): 659–69. <https://doi.org/10.2983/035.030.0308>.
- Waltham, N. J., and M. Sheaves. 2018. "Eco-Engineering Rock Pools to a Seawall in a Tropical Estuary: Microhabitat Features and Fine Sediment Accumulation." *Ecological Engineering* 120 (September): 631–36. <https://doi.org/10.1016/j.ecoleng.2018.05.010>.
- Whitman, E. R., and M. A. Reidenbach. 2012. "Benthic Flow Environments Affect Recruitment of *Crassostrea Virginica* Larvae to an Intertidal Oyster Reef." *Marine Ecology Progress Series* 463 (August): 177–91. <https://doi.org/10.3354/meps09882>.
- Wieczorek, S. K., and C. D. Todd. 1998. "Inhibition and Facilitation of Settlement of Epifaunal Marine Invertebrate Larvae by Microbial Biofilm Cues." *Biofouling* 12 (1–3): 81–118. <https://doi.org/10.1080/08927019809378348>.
- Yang, W., N. Kashani, X. W. Li, G. P. Zhang, and M. A. Meyers. 2011. "Structural Characterization and Mechanical Behavior of a Bivalve Shell (*Saxidomus Purpuratus*)." *Materials Science and Engineering: C* 31 (4): 724–29. <https://doi.org/10.1016/j.msec.2010.10.003>.